

FCH JU Grant Agreement no.:	245113
Project acronym:	KEEPEMALIVE
Project title:	Knowledge to Enhance the Endurance of PEM fuel cells by Accelerated Lifetime Verification Experiments
Funding scheme:	Collaborative Project
Area:	SP1-JTI-FCH.3 Stationary Power Generation & CHP
Start date of project:	01.01.2010
Duration:	42 months
Project Coordinator:	SINTEF (NO)

Deliverable Report:

Design Guide

D 1.5

Author (partner):	Laila Grahl-Madsen (IRD)
Other authors:	Thor Anders Aarhaug, Luis Colmenares, Steffen Møller-Holst (SINTEF)
Work package:	WP1, From Real-life operation to experimental program
Work package leader (partner):	Laila Grahl-Madsen (IRD)
Date released by WP leader:	2013-08-31
Date released by Coordinator:	2012-08-31

Dissemination level		
PU	Public	X
PP	Restricted to other programme participants (including the Commission Services)	
RE	Restricted to a group specified by the consortium (including the Commission Services)	
CO	Confidential, only for members of the consortium (including the Commission Services)	



Knowledge to Enhance the Endurance of PEM fuel cells by Accelerated Lifetime Verification Experiments

*Experiences from a comprehensive
PEMFC degradation study as basis for
Lifetime Prediction Modelling (D5.3)
and a Corresponding
Design Guide (D1.5)
for PEMFC degradation studies*

Public Deliverables 1.5 & 5.3*

**The merger of the two deliverables (D5.3 and D1.5) is agreed with Project Officer Mirela Atanasiu.*

The project:

The KeePEMAlive project has received funding from the European Community's Seventh Framework Programme (FP7/2007-2013) for the Fuel Cells and Hydrogen Joint Technology Initiative under Grant Agreement no.: 245113. The project was conducted by a consortium of European R&D institutions and companies with high expertise and long experience in the field. The involved industry partners possess advanced production capabilities enabling them to develop new improved Membrane and Electrode Assembly (MEA) materials as well as assembling and testing of PEM stacks and systems. The R&D partners are well equipped for material as well as cell and system performance characterization and provide expertise in statistical data analysis both from laboratory scale single cell, stack testing as well as real life system operation through related field tests in Denmark and France.

Table of Contents

Table of Contents	2
Acronyms	4
1 Introduction	5
2 Factorial designed experiments to reduce the work load.....	6
3 Real life fuel cell field testing to ensure relevance	7
3.1 Implementation of μ CHP systems in households	7
3.2 Assessment of real stack performance data	8
3.2.1 Data logging frequency	8
3.2.2 Evaluation of individual cell voltages in stack	8
3.2.3 Comparison of ex-situ characterisation and performance data	10
3.2.4 Calculation of stack degradation rates	12
3.2.5 Stochastic failure modes	14
4 Accelerated Stress Testing of Single Cells	16
4.1 Overview of single cell tests conducted	17
4.2 Recommended Break-in Procedure for single cells	17
4.3 AST stable operation parameter verification	18
4.4 Polarization characterization – frequency, # points and reporting	20
4.5 Single cell AST protocols.....	21
4.5.1 Continuous operation.....	21
4.5.2 Reformate operation	21
4.5.3 Fuel Starvation.....	23
4.5.4 Electrical Load Cycling	24
4.6 Assessment of results from the Fuel Starvation AST protocol	25
4.6.1 Calculated effects of main operation parameters on BoT cell performance	26
4.6.2 Calculated effects using #Cycles as response	28
4.6.3 Calculated effects using decay rate as response	29
4.6.4 Interactions of variables in modelling.	30
4.6.5 Ex-situ analysis of MEA materials subject to ASTing	30
4.6.6 Calculated effects of main operation parameters on Ru:Pt ratio.....	32
4.6.7 Current density distribution from segmented cell investigation	35
4.6.8 Comparison between fractional 2^{3-1} and full factorial 2^3 experiment	37

5	Accelerated Stress Testing of Stacks.....	39
5.1	Stack Initialisation	39
5.2	Stack test configuration	39
5.3	Test parameters.....	39
5.3.1	Continuous operation with hydrogen dead-end circuit.....	39
5.3.2	Continuous operation with open-end fuel circuits	41
5.3.3	Start/stop – idle mode stack test protocols.....	41
6	Lifetime Prediction Modelling	44
6.1	The initial strategy for KEEPEMALIVE.....	44
6.2	Literature on lifetime prediction	44
6.2.1	Lifetime prediction in batteries.....	44
6.2.2	Lifetime prediction in fuel cells.....	45
6.3	Lifetime modelling in KEEPEMALIVE	46
7	Summary of Experiences from the project	49
8	Recommendations for degradation studies.....	51
9	References	53

Acronyms

AST	Accelerated Stress Test
BoL, / BoT	Beginning of Life / Beginning of Test
CHP	Combined Heat and Power
CL	Catalyst Layer
CVMS	Cell Voltage Measurement System
DoW	Description of Work
ECSA	ElectroChemical Surface Area
EDX	Energy Dispersive X-ray analysis
EoL / EoT	End of Life / End of Test
EW	Equivalent Weight (used for polymer membranes)
GA	Grant Agreement
GDL	Gas Diffusion Layer
IEC	Ion Exchange Chromatography
JM	Johnson Matthey
LSV	Linear Sweep Voltammetry
LT PEMFC	Low Temperature Proton Exchange Membrane Fuel Cell
MEA	Membrane Electrode Assembly
MoT	Middle of Test
OCV	Open Circuit Voltage
ORR	Oxygen Reduction Reaction
P	Pressure
PFSA	PerFluorinated Sulphonic Acid
PTFE	PolyTetraFluoroEthylene
RSD	Relative Standard Deviation
RH	Relative Humidity
rf	Reinforced
SD	Shut Down
SEM	Scanning Electron Microscopy
SU	Start Up
SWC	Squared Wave Cycling
T	Temperature
TEM	Tunneling Electron Microscopy
TGA	Thermo Gravimetric Analysis
TKK	Tanaka Kikinzoku Kogyo
TWC	Triangular Wave Cycling
WE	Working Electrode
WP	Work Package
XRD	X-Ray Diffraction

1 Introduction

Fuel cells are expected to play a crucial role in the sustainable energy system of the future. Combined Heat and Power (CHP) constitutes a potential market segment for fuel cells. However, high cost and limited durability represent two remaining key challenges to be solved prior to large scale market introduction of Proton Exchange Membrane Fuel Cells (PEMFCs). Whereas cost is less demanding, the durability requirements are especially stringent for CHP applications.

The KeePEMalive project is focusing on PEMFCs for residential applications in the micro (~kW) range (μ CHP) and the main objectives have been the establishment of:

- *improved understanding of degradation & failure mechanisms for stationary PEMFCs, with special focus on μ CHP applications and*
- *accelerated stress test (AST) protocols, a sensitivity matrix and a lifetime prediction model for stationary μ CHP applications*

- thereby contributing to reaching the durability target for CHP applications of 40 000 hours.

The topic "degradation of fuel cells" is complex in its nature. The transport processes and likewise the degradation mechanisms taking place in PEMFCs are highly depending on the materials in use as well as the operating conditions.

To take into account the complexity and interrelations, a systematic approach to the experimental design of the accelerated stress test (AST) program was taken in the KeePEMalive project, as briefly summarized in Chapter 2.

To ensure the relevance of the studies on durability, a link to two demonstration field tests was established. Statistical analysis of Real life stack data reveal interesting relationships and clearly underpin the fact that degradation is a distribution as demonstrated by the population of cell voltages in a stack. This distribution changes significantly with time from normal to a Weibull-like shape as discussed in Chapter 3.

The majority of the effort in the KeePEMalive project has been devoted to carry out a comprehensive Accelerated Stress Test (AST) program. An immense amount of data has been generated as a result of experiments carried out in 7 laboratories and assessment of 6 AST selected protocols for single cell testing mirroring stationary μ CHP applications. During revision of the AST program, the number of protocols was reduced to 4, and details for these are summarized in Chapter 4. To exemplify the findings, results from the AST protocol on Fuel Starvation and the analysis thereof are presented and discussed in detail in Chapter 4. Similarly, details for AST protocols for stacks are provided in Chapter 5.

A thorough assessment of available literature on the relationships between operation conditions and lifetime issues was carried out at an initial stage of the project. Key factors such as temperature, humidity, fuel composition, current density and transients are interrelated. So far, however, the majority of scientific studies on degradation reported in literature have been focusing on one factor at a time as discussed on Chapter 6.

Therefore, in this project the ambition has been to reveal and quantify these interrelationships, by utilising statistically designed experiments. However, it turned out that while the project simultaneously had the ambition of improving the materials under study, challenges were encountered with respect to achieve statistically significant results. A summary of these challenges and the ways to corrective actions taken to get around these obstacles, are summarized in Chapter 7.

Based on this, recommendations for experimental test programs on PEMFCs for μ CHP applications are provided in Chapter **Error! Reference source not found.**

2 Factorial designed experiments to reduce the work load

As may be inferred from the introduction in Chapter 1 on the complexity of PEMFC degradation processes, it is evident that the work load of mapping all possible variations in operation parameters and the corresponding effect on degradation is immense. Therefore, a systematic approach was taken to facilitate statistical analysis through factorial design¹.

The main benefit from using factorial design is that the multivariate approach allows for an efficient way to simultaneously evaluate the effect of several input variables. As an example, evaluation of three variables at two levels requires 24 experiments when varying one variable at a time. In a 2^3 experimental design, three variables at two levels can be fully interpreted in 8 experiments. Both main effects of variables as well as interaction between variables can be quickly found using simple (i.e., Yates) algorithm. Further, in a traditional one variable at a time approach, no information about interaction is gained. In this way, optimum response is not secured; the maximum might be local and not global.

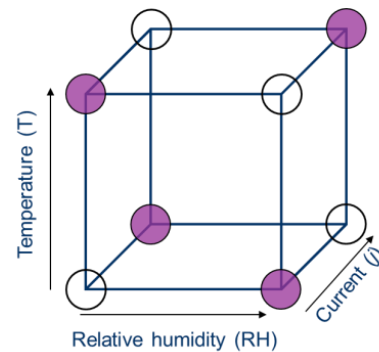


Figure 1 Factorial design for studying 3 factors at 2 levels.

By carefully designing the Accelerated Stress Test (AST) program the experimental workload was reduced significantly to a manageable level. Based on the real life field test of μ CHP fuel cell systems (Section 3.1), the main operation variables (factors) selected were temperature (T), relative humidity (RH), and current density (j). By varying these systematically, the interactions between main factors were identifiable.

A 2^3 factorial design is comprised of two identical subsets of $2^{3-1} = 4$ experiments. In these subsets, main effects cannot be discerned from two-way interactions. These so-called fractional factorial designs are useful for screening purposes, and can be extended to a full 2^3 when required.

The drawback for factorial designs is that the number of required experiments is cut to a minimum. Thus, all experiments must be completed. If not, the resulting data are unresolved in the variables used and the Yates' algorithm is useless.

A requirement for factorial designs is orthogonality: all input variables must be independent of each other. A 2^3 experiment can be illustrated by a cube where all angles are 90° (Figure 1). The experiments make up the corners of the cube. The two subsets of experiments, here illustrated by transparent and purple balls, for tetrahedrons the optimally span the cube.

¹ Box, Hunter and Hunter, *Statistics for Experimenters - An introduction to Design, Data Analysis and Model Building*, Wiley, ISBN 0-471-09315-7, 1978

3 Real life fuel cell field testing to ensure relevance

3.1 Implementation of μ CHP systems in households

In the initial phase of the KeePEMalive project, typical operation characteristics for the residential μ CHP application were mapped, and based on this six key stressors were identified, resembling conditions that these fuel cells typically experience in real life during all seasons. Both natural gas (NG) and pure hydrogen were assessed as fuel for the systems in the Accelerated Stress Test program (Chapter 4), due to the link to two field tests, one at Lolland in Denmark (Figure 2, pure H_2) and a French field test at 4 locations all using NG as fuel and reformer technology.



Figure 2 Field test at Vestenskov, Denmark, at which in total 32 PEMFC based CHP systems have been deployed in households, from which real life data has been fed into the KeePEMalive project for comparison to accelerated stress tests.

Assessment of the field data from real life operations (at Lolland) related to the KeePEMalive project has enabled the project system development partner IRD to improve the μ CHP system and take the technology one step closer to fulfil the stringent requirements for long term durability. By exchanging some MEA precursors and further optimise the operational conditions in the Danish on-going field test the MEA durability was increased significantly e.g., the degradation rate was decreased five-fold from 20 to 4 μ V/h, corresponding to increasing the system lifetime from the previous level of 3 500 hours to an expected 17 000 hours (~2 years). The heat and electricity demand and the related energy and emission savings from utilizing the CHP-units in Danish households have been mapped for various seasons and during the course of the project the electric system efficiency has been improved to 50%.



Figure 3 Example of field test installation in one of the households in Vestenskov, Denmark.

3.2 Assessment of real stack performance data

Stack performance data from the Vestenskov field tests in Denmark was assessed statistically and results are reported in this section.

3.2.1 Data logging frequency

For stacks, logging frequencies higher than $\sim 1/60$ Hz generally produce large amounts of data when individual cell voltage monitoring system (CVMS) is enabled. This makes processing of data over large time intervals difficult or requires extensive processing power/time. The applied logging frequency could also be excessive: the resolution of the voltage monitoring system dictates to some extent the maximum frequency required.

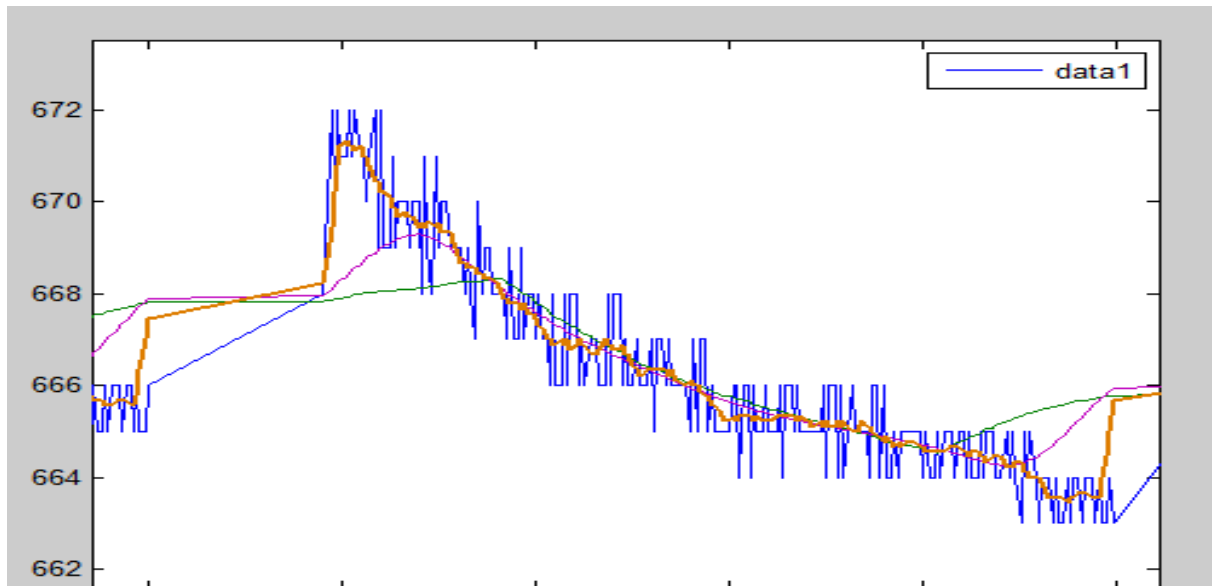


Figure 4. One (1) Hz data log of cell voltage of stack. Raw data (blue) compared to smoothing by floating average windows of 10 (orange), 100 (magenta) and 1000 data points (green).

As seen from Figure 4, the resolution of the CVMS is 1 mV. Reducing the logging frequency to 0.1 Hz (orange) would still contain the noise, but the noise could not be resolved by fitting data. Simple smoothing of data effectively removes noise. The downside is the processing power required to smooth the data. If processing power is available, robust data processing with exclusions of outliers could be applied in order to maintain as much scope in the original data as possible.

3.2.2 Evaluation of individual cell voltages in stack

In order to assess the precision in data used for calculation of degradation rates and lifetime prediction, more than one measurement is required. Optimally, a population of identical stacks running under identical ambient and operational conditions should be available for statistical evaluation. This is rarely the case. For a single stack, the individual cell voltages can be utilized in order to evaluate the variance. More interesting than the average cell voltage and its corresponding standard deviation is the distribution of the population.

Stack geometry will affect the distribution of individual cell voltages. From a design point-of-view, it is of interest to evaluate individual cell degradation rates in order to verify stack design. From evaluation of individual cell voltages in the stack, deviation in the end cells were observed. Therefore, the two outermost cells at each end of the stack were excluded from further cell voltage evaluation. So, in this particular exercise, 43 cells were used to evaluate the population distribution. In order to improve distribution assessment, 1 Hz data was used where 200 seconds of individual cell voltages were used

to create voltage populations. At Beginning of Test (BoT), the distribution is best described normally, as shown in Figure 5.

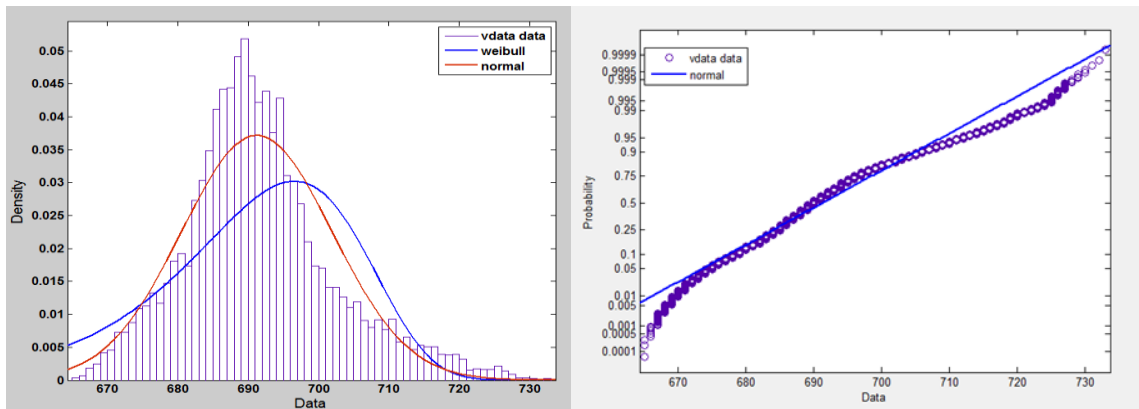


Figure 5. Probability density (left) and probability (right) plots for BoT data (November 2011).

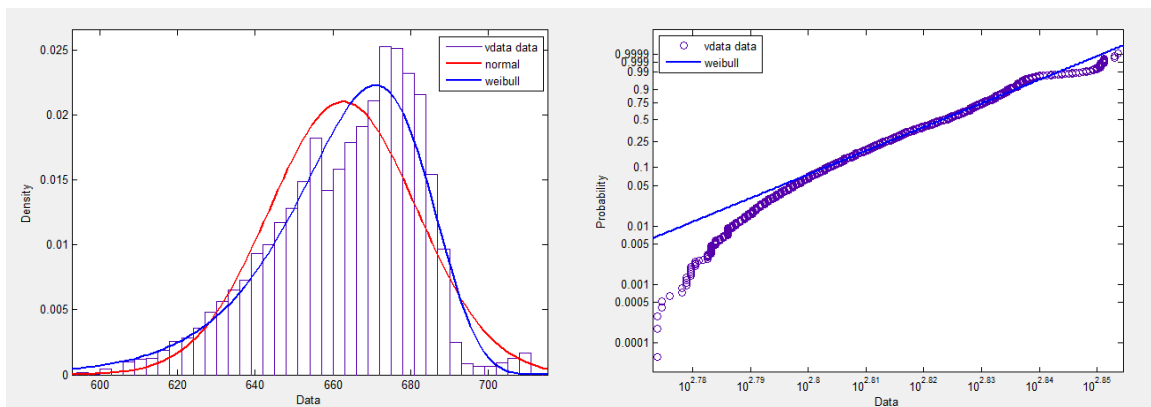


Figure 6. Probability density (left) and probability (right) plots in June 2012.

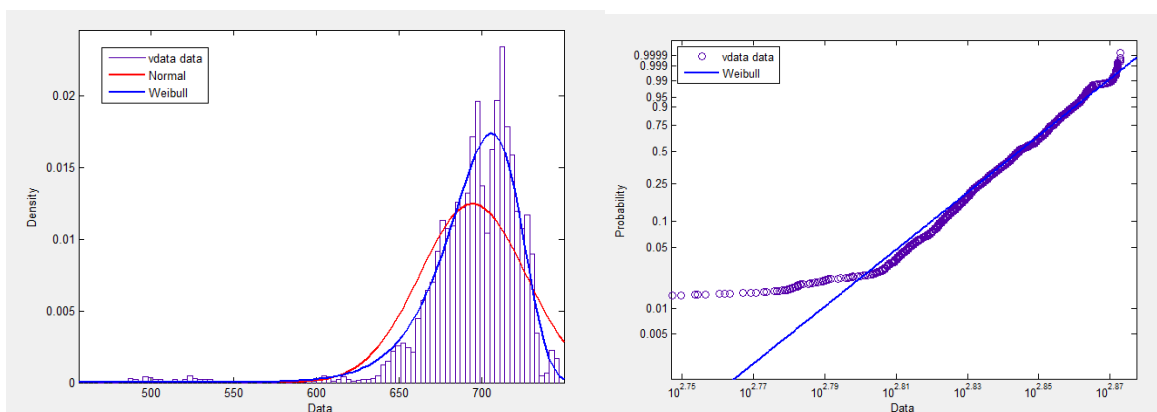


Figure 7. Probability density (left) and probability (right) plots in July 2012. Data taken from 20 A load due to reduced heat demand from stack in summer.

The probability density is better described by a normal distribution, symmetric about the mean value. The goodness of fit can be evaluated numerically e.g., by a log likelihood parameter. As seen from both plots, some cells with high performance deviate from the normal distribution. Data from the same stack at in June 2012 is shown in Figure 6.

Clearly, the symmetry about the mean value is diminishing as more and more cells have reduced performance producing a "tail" from the lower side of the mean. In July 2012, the tail gets even more pronounced as shown in Figure 7.

The tailing off of individual cells has become very high. As can be seen from Figure 7 (right), even a "shapeable" Weibull distribution does not fit the tail well.

The Weibull distribution has seen many applications in product life studies. Unlike the normal distribution, where a uniformly increasing failure rate is observed, the Weibull distribution has a shape parameter that allows for tuning of the failure rate. The Weibull probability density function is given by:

$$f(y) = \left(\frac{\beta}{\alpha}\right)y^{\beta-1}e^{-\left(\frac{y}{\alpha}\right)^\beta}$$

where β is the shape factor for the distribution. α is the scale parameter, often called characteristic life. It is always the 63.2th percentile of the population and has the same unit as time, y .

Based on the discussion above, it was postulated that a check for normality in single cell voltage distribution for a running stack could say something about the state of health for the stack. A normal Chi-Square test was used to evaluate the "degree of normality". The result is shown in Figure 8.

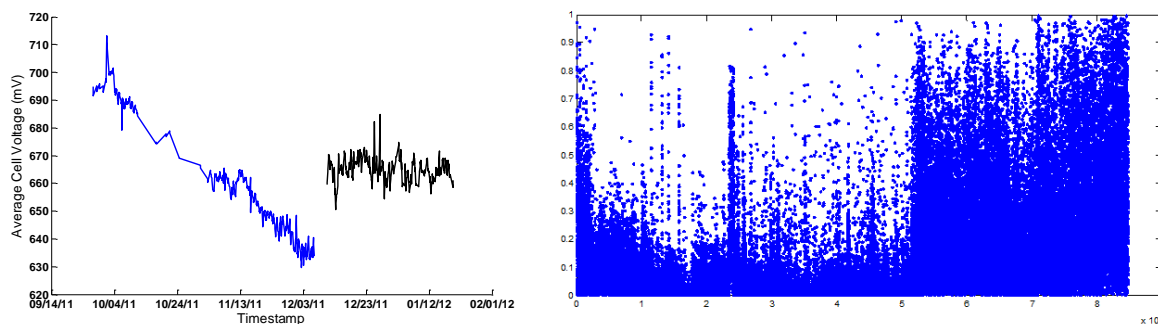


Figure 8. Smoothed average cell voltage (left) before (blue) and after (black) change in stack operating conditions. The Chi-Square test score for normality is shown to the right, higher score indicating a more normal distribution.

The figure shows how severe voltage decay over time was remedied by a change in operating conditions. A check for normality (Figure 8, right) reveals that approximately half the readings pass as being normally distributed according to the test. By plotting the test scores, it becomes obvious that more normality in the data distribution is observed when the stack is running at "healthy operating conditions".

3.2.3 Comparison of ex-situ characterisation and performance data

Stack geometry and gas manifolding are both of key importance for the performance of the stack. Moreover, hardware design is to a large extent dictating the variations between the individual cells in the stack. Even geometric orientation of the stack affects the performance and must be taken into account when performance is evaluated. For a particular stack three MEAs in use were evaluated post mortem by SEM microscopy:

- Cell 1: "Cold/bottom"
- Cell 13: Cross-over development early in life
- Cell 40: Well performing cell

Areas from anode inlet, middle and anode outlet were evaluated by measuring electrode and membrane thicknesses. The results were inconclusive due to large variance in the thickness along the cross-sections. A general trend, however, was that both electrode thicknesses were reduced closer to the outlet (Figure 9) whereas the membrane thickness showed an opposite trend.

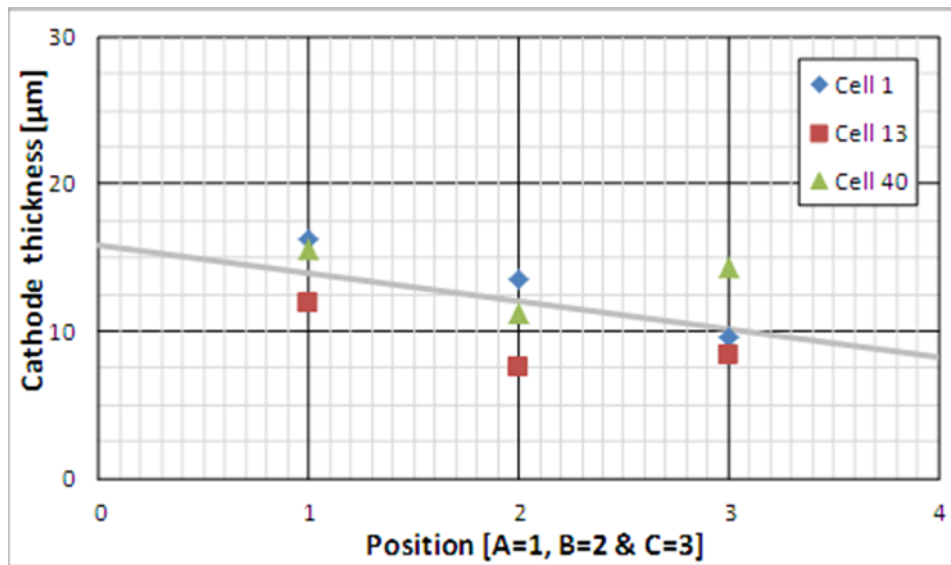


Figure 9. Cathode thickness assessment by SEM. Positions investigated is anode inlet (A), middle (B) and outlet (C).

The SEM micrographs showed to a larger extent migration of Pt into the membrane for Cell 13. The diffusion of both hydrogen and oxygen gases into the membrane and the inherent recombination at the Pt-sites present, may explain the creation of pinholes for this cell. The cross-over of Cell 13 was easily discoverable from the typically faster drop in OCV when the stack was set to idle mode in addition to a low performance due to a mixed cathode potential. As the monitoring of the voltage transient to idle mode is challenging, other and simpler ways to detect cross over were explored.

By recording the lowest voltage of any cell for each log line from the CVMS, the count of minimum voltages should reflect the performance of the cell. The total counts for cells under load are shown in Figure 10.

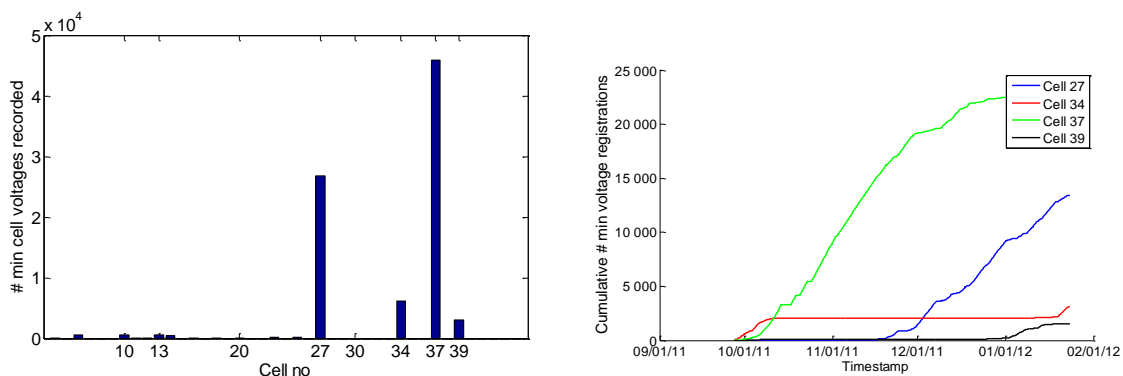


Figure 10. Total and cumulative minimum cell voltage counts for cells under load ($I > 49.5 \text{ A}$).

Clearly, four cells perform significantly worse than the others. The cumulative plots give information about the performance over time. The weakness of the method is that it's discrete: only one cell can record the lowest value at a time. It's seen that Cell 34 has bad performance early, whereas Cell 39 starts to lose performance later in stack life. The cross-over of Cell 13 is not reflected in this dataset. As it is expected that the impact of H₂-crossover is less at high current density as more fuel is consumed at the anode, the same exercise was performed at stack idle mode as shown in Figure 11.

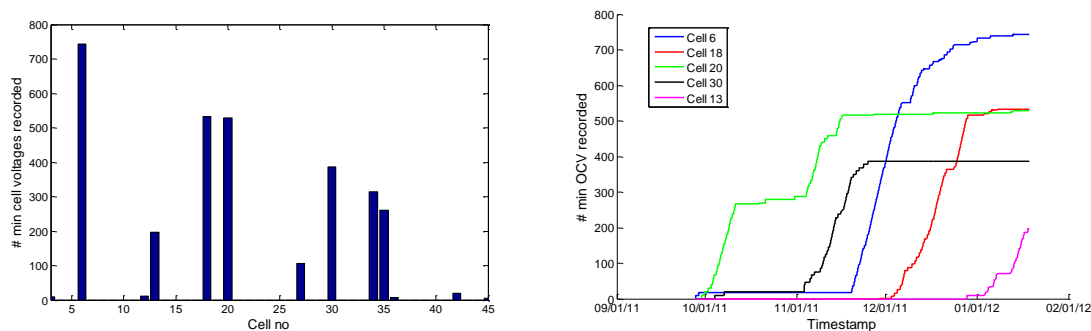


Figure 11. Total and cumulative minimum cell voltage counts for cells in idle mode.

At OCV conditions, a more even distribution of minimum cell voltages was observed. Here, Cell 13 is amongst the top eight contributors to minimum OCV. The cumulative plot only shows Cell 13 to have low OCV performance late in stack life. Cell 13 was initially tagged and identified as having developed cross-over early.

It appears that the evaluation of cross-over does not correlate well with minimum performance data, neither at OCV or nor during load. Hence, it might be concluded that other means to assess the transients of operation change from load to idle must be used for early detection of individual cell cross-over as potential a precursor for pin-holes and eventually cell failure.

3.2.4 Calculation of stack degradation rates

There are many ways to estimate the performance degradation rate of a fuel cell stack. The estimates obtained are strongly dependent of which and how data are fitted. Some reversible (recoverable) degradation effects are typically encountered (e.g., flooding/dehydration/CO-poisoning), and these should preferably be separated from irreversible degradation when calculating degradation rates. For automotive applications, data from high and varying load with minor contribution from reversible contribution can be utilized. For stationary applications, data are mainly available from nominal operation and during idling. Depending of the nature of reversible degradation, however, the reversible contribution to voltage loss may under most operation conditions be assumed to be constant, and hence will not contribute when degradation rates are calculated. An example of a stack exhibiting reversible degradation is shown in Figure 8. Upon changing the operation conditions, the average cell voltage decay was neutralized and a completely different lifetime estimate at the "new" operating conditions may be calculated.

Moreover, strategies to mitigate cell degradation may include a series of aspects, including a systematic change in operation conditions to compensate for inherent material changes encounter during long term stack operation. This may be exemplified by changes in the backing material's hydrophobicity/hydrophilicity (altering the contact angle) causing increased adhesion of water droplets in the porous structure. To mitigate such changes one may need to increase the air stoichiometry after

a given time of operation, thereby prolonging the lifetime of the stack, as defined by the maximum acceptable performance loss.

Stack performance data typically exhibit two distinct regions of very different degradation rates as illustrated in Figure 12.

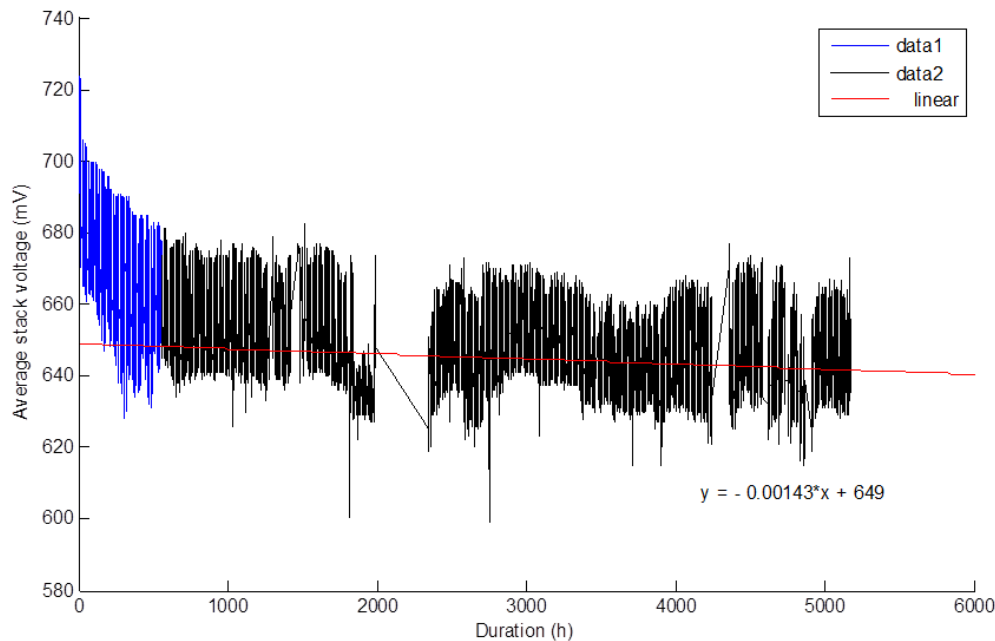


Figure 12. Average cell voltage data at load $I > 49.5$ A. Linear regression gave estimates of degradation of -53 and $-1.4 \mu\text{V h}^{-1}$ for the data1 (blue) and data2 (black) regions, respectively.

By dividing data into two blocks, degradation rates can be found by linear regression. The rates are substantially different. Although not an End-of-Life test criterion per se, 10 % stack performance loss is often used when evaluating stack durability. When estimating an initial stack average voltage of 675 mV, the average cell voltage would reach the 10 % performance loss mark after 28 963 hours.

The correlation between the performance loss metric and predicted lifetime is shown in Figure 13. In order for the stack to reach its durability target of 40 000 hours, a performance loss of 12.5 % must be allowed. As long as the Balance of Plant (BoP) and auxiliary system is dimensioned to accommodate this, a 12 % loss may easily be acceptable, especially for a μ -CHP-system for which both the electricity and the heat is utilized.

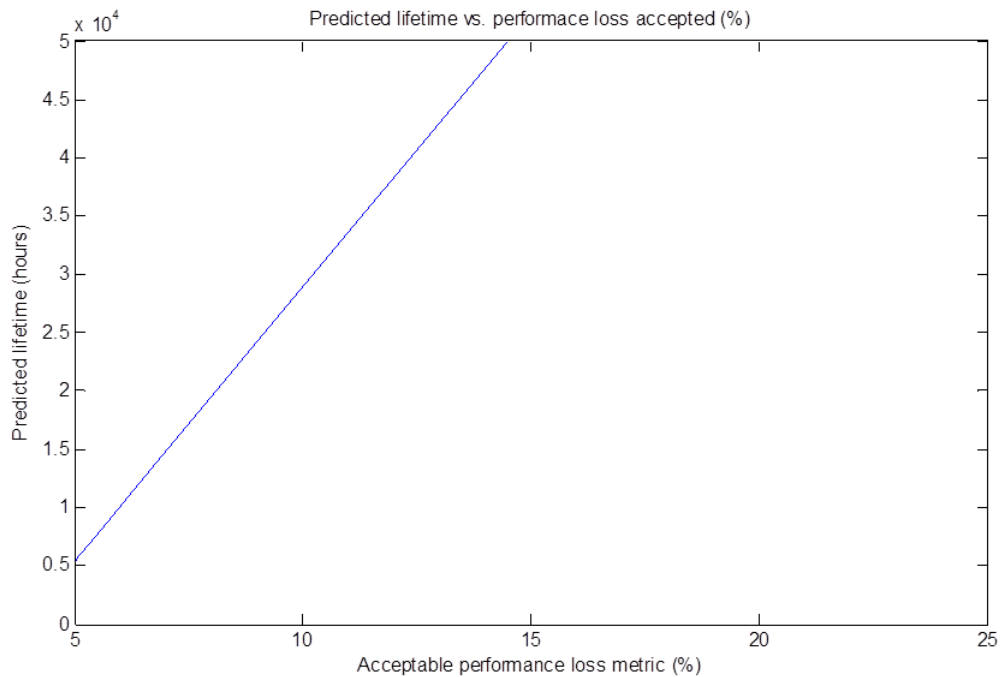


Figure 13. Predicted lifetime (in 10 000 hours) vs. accepted performance loss (%).

Small changes in the degradation rate obtained from 5000 hours of operation greatly affect the projected estimated performance after 40 000 hours. It is therefore essential to establish knowledge of the variance of these estimates.

3.2.5 Stochastic failure modes

Estimation of system lifetime from performance data is severely limited by the fact that there are many failure modes in fuel cells that are not reflected by performance. A good example is the development of localized hydrogen cross-over typically linked to inhomogeneities or weak points generated during material production or MEA assembling, eventually leading to pin-holes. The failure of single cells in stacks has been shown to be of a stochastic nature. The linear extrapolation of voltage decay rates into the future does not take into the account that the probability of cell failure increases with time.

One approach to incorporating the stochastic failure modes in lifetime prediction modelling is to apply population statistics. By fitting actual or accelerated stress test data to population distribution models, the probability of failure can be estimated.

The Cumulative Hazard Function, $H(x)$, can be interpreted as the probability of failure at time x . Assuming a normal distribution of life times, here shown in Figure 14, the probability of failure increases uniformly with time.

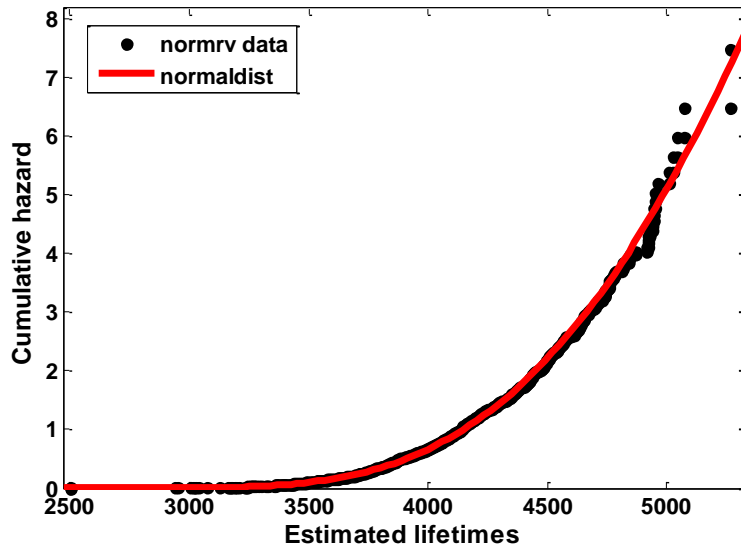


Figure 14. Cumulative hazard plot for a simulated population of PEMFC stack lifetimes with average 4000 hours and a standard deviation of 400.

For a Weibull distribution, the cumulative hazard function is a function of the shape parameters shown in Figure 15.

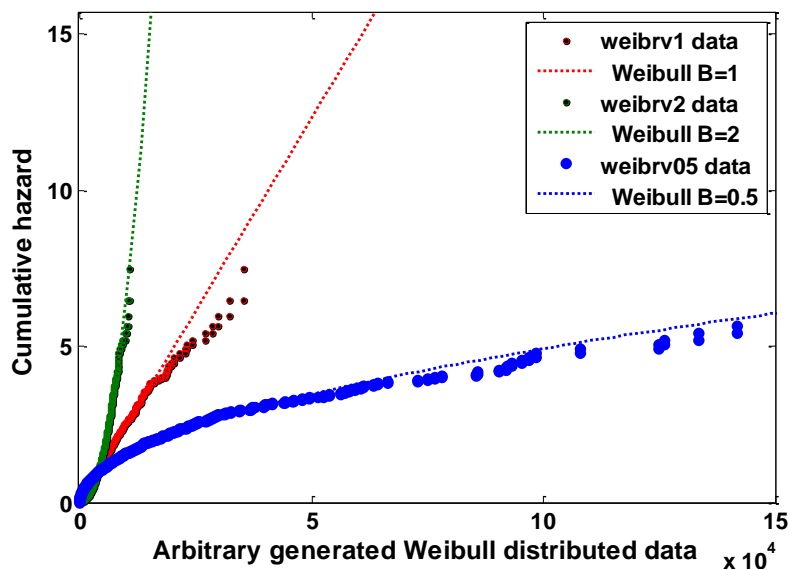


Figure 15. Cumulative hazard fits of randomly generated Weibull population data with shape parameter $B=0.5$ (blue), $B=1.0$ (red), $B=2.0$ (green).

The ability to shape the probability of failure with time to fit actual failure data makes the Weibull distribution very useful in product reliability studies. For PEMFC stacks, very little data has been reported. In order to use population statistics for lifetime estimation, lifetime data must be fitted to a Weibull distribution. From these fits, the shape parameter and the cumulative hazard function can be obtained. These aspects will be further elaborated upon in one of the planned publications.

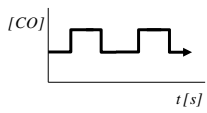
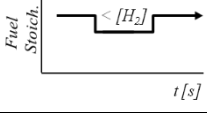
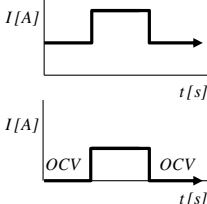
4 Accelerated Stress Testing of Single Cells

Adequate electrochemical characterisation techniques were evaluated and selected for a comprehensive Accelerated Stress Test (AST) program including determination of ElectroChemical Surface Area (ECSA), Electrochemical Impedance Spectroscopy (EIS), Cyclic Voltammetry (CV) etc.

The following four (4) situations are highlighted as key stressors under typical stationary PEM fuel cells operating conditions (Table 1):

- *Continuous operation (simulates winter μ CHP profile)*
- *Reformate operation (CO exposure)*
- *Fuel starvation (hydrogen supply variation)*
- *Electrical load cycling (representing Fall / Spring μ CHP profiles, OCV cycling – summer μ CHP profile)*

Table 1 List of stressing conditions that are evaluated applying AST under specified operating mode and variable test conditions

Stressing Situation	Accelerated Stress Test (AST)	Operation Mode	Variable Conditions
Continuous Operation 	Water Management (i.e. 'Flooding'), μ -CHP winter profile	Constant Current Density Operation - monitoring cell voltage	Cell Temperature Relative Humidity Current Density # of characterizations
Reformate Operation 	CO exposure	Constant Current Density Operation - pulse wise feed of 20 ppm [CO]	Cell Temperature Air bleed CO pulses (on/off)
Fuel Starvation 	Sub-stoichiometric Hydrogen Supply	Constant Current Density Operation - cycled anode (sub-) stoichiometry	Current Density Relative Humidity Cell Temperature
Load Cycling 	Load Cycling (i.e. μ -CHP fall profile, μ -CHP spring profile) OCV cycling (μ -CHP summer profile)	Switch between low and high or 0 and medium Current Density	Relative Humidity Current Density levels Cell Temperature

4.1 Overview of single cell tests conducted

Around 100 Membrane and Electrode Assemblies (MEAs) were studied during the AST program accumulating more than 20 000 single cell test hours. Supplemented by stack testing, this has revealed by statistical analysis, the most detrimental operating conditions causing degradation and cell failure.

A considerable database of test results has been built up linking degradation rates to single cell operation conditions. Based on more than 32 single cell experiments (complete 2^3 set) under different stressing operation conditions (Table 2); statistical data analysis has shown that the presence of CO (arising from NG reforming) in the fuel, the relative humidity (RH) level and the operating temperature (T) of the cell are the key factors affecting performance degradation. Replicates have been used to estimate standard deviations and thereby enabled determination of the significance of the results.

Table 2 Conducted experiments at single cell level during the phase II of the project

Stressing situation	Variable Conditions	No. Exp. performed applying revised AST
Continuous operation	a) Cell Temperature b) Relative Humidity c) Current Density	8 (complete 2^3 set)
Reformate operation	a) Cell Temperature b) Air bleed content c) Current Density	8 (complete 2^3 set)
Fuel Starvation	a) Cell Temperature b) Relative Humidity c) Current Density	9 (complete 2^3 set + 1 replicate)
Load cycling	a) Cell Temperature b) Current Density levels c) Cycling frequency	12 (complete 2^3 set + 2 replicates + 2 at diff. cycling frequency)

4.2 Recommended Break-in Procedure for single cells

A good break-in procedure is a prerequisite for reliable results. The following break-in procedure is recommended: Cycling between 0.35 and 0.75 V at 10 minute intervals for four (4) hours, at 65°C and 80% RH, followed by at least 12 hours constant current (0.4 A/cm²) operation. Out of convenience, the Beginning of Test (BoT) shall be anywhere between 16 to 24 hours after the break-in procedure commenced. Following this break-in procedure the cell performance shall, for comparison, be evaluated at the break-in conditions (65°C and 80% RH), prior to adjusting the operation parameters to the actual operation conditions for starting the individual ASTs. The performance characterization at BoT conditions shall then be performed under the specific AST protocol operation parameters!

4.3 AST stable operation parameter verification

A prerequisite to succeed with the interpretation of results from ASTs is the ability to run all experimental conditions. If a certain combination of operation parameters leads to operation instabilities (*i.e.*, flooding and de-hydration), the parameter settings must be adjusted accordingly, to tune parameters and thereby enter the stable operation regime.

As an AST example, the continuous varying operation parameters are given in Table 3 and the parameter space is schematically depicted in Fig. 16. The sequence of how the operational stability of the Tests comprising Box 1 will be assessed is illustrated in Figure 17.

Table 3 The operation parameters for the 2^3 experimental design with the boxed sets indicated for the Continuous operation ASTs.

Test	T [°C]	%RH	Current Density	Box
1	65	40	0.2	1
2	65	40	0.6	2
3	65	80	0.2	2
4	65	80	0.6	1
5	85	40	0.2	2
6	85	40	0.6	1
7	85	80	0.2	1
8	85	80	0.6	2

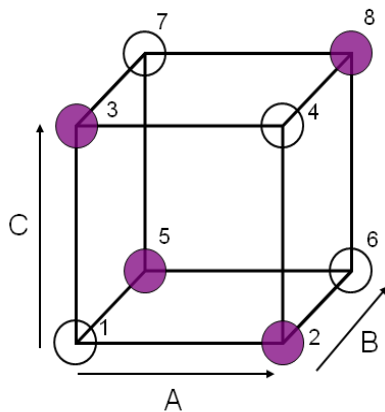


Figure 16

Schematic illustration of parameter space for the 2^3 experimental designs, as shown in Table 3. “A” corresponds to Current density, “B” to Temperature, and “C” to Relative Humidity. Box 1 (Table 3) is given by the open spheres, and Box 2 by the coloured spheres.

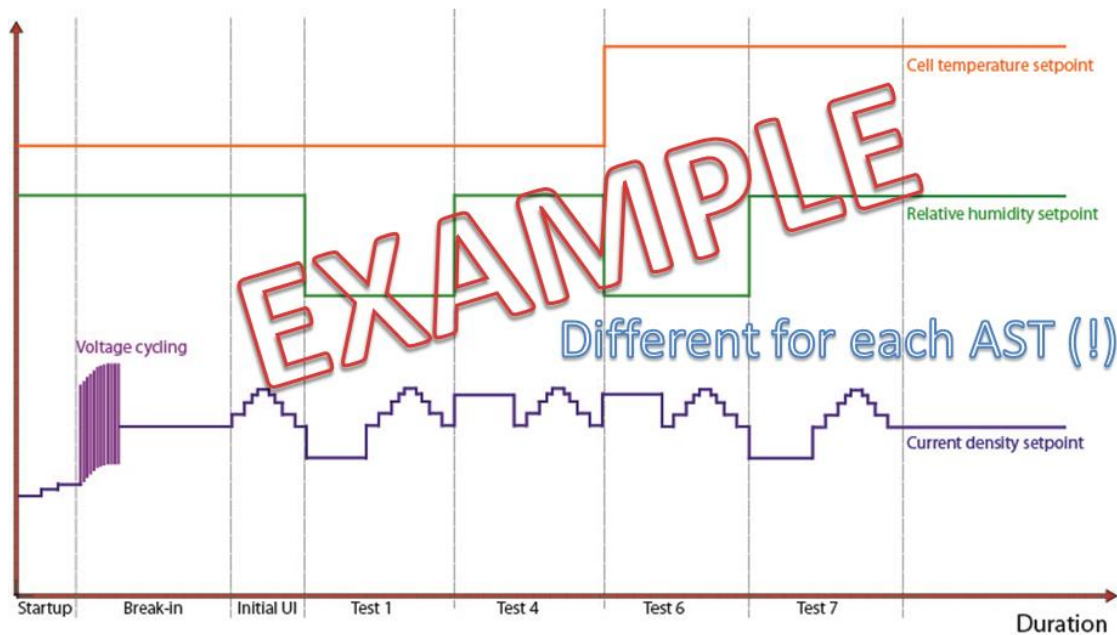


Figure 17 Sequence for evaluating operation parameter settings for the tests comprising Box 1 for the ASTs of the Continuous operation protocol. The operation parameters for each Test shall be kept stable for 2 hours prior to the UI-curve measurements to ensure stable performance, or alternatively reveal the potential unstable performance at these parameter settings, leading to re-adjustment of operation parameters.

Key points on the execution of the operation parameter verification experiments:

- 1) The Break-in procedure, as described in Section 4.2, shall be followed.
- 2) An Initial UI curve at the Break-in operation parameter settings shall then be obtained.
- 3) Stable operation of at least two hours is required before the UI characterization for each Test is made. The time required to obtain "stable" voltage may vary between tests.
- 4) No characterizations other than UI curves are required. Six distinct points on the UI-curve are required identical to those that will be used every 24 h for the actual AST-protocols (Section **Error! Reference source not found.**).
- 5) The sequence of tests execution is not fixed (example provided in Figure 17). It may be convenient to choose a different sequence (*i.e.*, it may be easier to change RH set-point once then vary the temperature set-point) depending on your test station hardware specifications.
- 6) To induce a minimum of degradation it is recommended to minimize transients (*i.e.*, between Test 4 to 6, (Figure 17)) by changing set-points in steps.
- 7) It is an absolute requirement to test all eight (8) combinations of parameter settings (Box 1 and Box 2) as input for the assessment and confirmation of the high and low levels of the parameters for the AST. The two Boxed sets of tests could be performed subsequently, supplementing the Tests shown in Figure 17 (Box 1) with Tests 2, 3, 5 and 8 (Box 2), using the same MEA. In case of clear signs of degradation, a new, identical MEA shall be used.

4.4 Polarization characterization – frequency, # points and reporting

It is recommended to perform UI characterization every 24 hours at the operation conditions which are used for the specific AST, NOT going back to "standard" conditions. The rationale is as follows: With this 24 hours frequency, changes in operational set-points back to the "standard" conditions (65°C and 80% RH) every day will introduce gradients which will contribute significantly to degradation. The number of points for each UI curve shall be 6, chosen such that there are 2 points in the activation regions, 2 in the ohmic, and 2 in the mass transport region. To assure the 2 points in each region, the points are specified by the voltage (Table 4). A data logging frequency of ≥ 0.1 Hz is recommended.

Table 4 Voltage levels for the Polarization characterization each 24 hours for all AST-protocols including minimum time at each voltage. The potential hysteresis shall be revealed by measuring the Polarization curve both up and down. A minimum logging frequency of 0.1 Hz is required. To the right in the table, the format of UI-curve reporting is indicated [shaded cells].

Cell Voltage [V]	Duration [min]	Region of the Polarization curve	Average Current density [mA/cm ²]			Standard deviation Current density		
			Whole duration	Last 2 minutes		Whole duration	Last 2 minutes	
OCV	3	N/A		2 - 3			2 - 3	
0.85	3	Activation		2 - 3			2 - 3	
0.80	3	Activation		2 - 3			2 - 3	
0.60	5	Ohmic		4 - 5			4 - 5	
0.45	5	Ohmic / Mass transport limitations		4 - 5			4 - 5	
0.35	10	Ohmic / Mass transport limitations		9 - 10			9 - 10	
0.45	5	Ohmic / Mass transport limitations		4 - 5			4 - 5	
0.60	5	Ohmic		4 - 5			4 - 5	
0.80	3	Activation		2 - 3			2 - 3	
0.85	3	Activation		2 - 3			2 - 3	
OCV	3	N/A		2 - 3			2 - 3	

4.5 Single cell AST protocols

4.5.1 Continuous operation

The experimental conditions for the continuous operation AST protocol are listed in Table 5 & 6.

Table 5 Overview of the constant gas conditions before and during execution of the Continuous Operation AST protocols.

Input	Anode	Cathode
Gas supply	Hydrogen	Air
Stoichiometry	1.5	3.0
Backpressure	0.4 (1.4 bar total pressure)	0 (ambient pressure)

Table 6 Overview of the variable operating conditions before and during execution of Continuous Operation AST protocol.

Variables	Low Setting	High Setting
Current Density	200 mA/cm ²	600 mA/cm ²
Relative humidity, <u>Anode & Cathode</u>	40%	80%
Cell Temperature	65°C	85°C

4.5.2 Reformate operation

The constant conditions for the Reformate operation AST are shown in Table 7 and the variables in

Table 8.

Table 7 Overview of the constant gas conditions before and during execution of the AST protocol on Reformate operation.

Input	Anode	Cathode
Gas supply	Reformate fuel	Air
Relative humidity, Anode & Cathode	80%	
Stoichiometry	1.5	3.0
Backpressure	Ambient	Ambient
CO	20 ppm continuous flow	-

Table 8 Overview of variable operating conditions before and during execution of the AST protocol on Reformate operation.

Variables	Low setting	High setting
Air bleed	0%	3%
Cell temperature	65°C	85°C
Current Density	200 mA/cm ²	600 mA/cm ²

4.5.3 Fuel Starvation

The best results for simulating fuel starvation have been obtained with constant gas supply and variation of the current load which leads to lower gas stoichiometries ($\lambda < 1$). The cells are operated with a current density of 200 mA/cm² at the low setting (400 mA/cm² at high setting) at constant gas flows according to a stoichiometry of 1.5 for hydrogen and 3 for air in the recovery interval. The starvation interval is performed by increasing the current load to 333 mA/cm² and 666 mA/cm² respectively, resulting in a hydrogen stoichiometry of 0.9. The conditions for this AST protocol are shown in Table 9 &

Table 10.

Table 9 Overview of the constant gas conditions before and during execution of the Fuel Starvation AST protocol.

Input	Anode	Cathode
Anode stoichiometry	0.9 for 10 seconds (fuel starvation) then 1.5 for 3 min (recovery)	
Gas supply	Hydrogen	Air
Backpressure	0.4 bar (1.4 bar total pressure)	Ambient (no backpressure)

Table 10 Overview of variable operating conditions before and during execution of the Fuel Starvation AST protocol.

Variables	Low setting	High setting
Relative humidity, cathode & anode	40%	80%
Cell temperature	65°C	85°C
Current Density	200 mA/cm ²	400 mA/cm ²

4.5.4 Electrical Load Cycling

The aim of including this protocol was to highlight the influence of Fall & Spring period in typical μ CHP operation, i.e., high load frequencies typically once a day. Critical variables are temperature, relative humidity and frequency of load change.

Current density is cycled between 200 and 600 mA/cm² (Mode cycle 1) and between 0 and 400 mA/cm² (Mode cycle 2) in order to evaluate the effect of excursions to OCV.

Under these conditions the amount of liquid water in the system will change affecting the mass transport, and the transient in potential at the cathode. Different duration of the voltage hold may also affect catalyst (support) properties and stability.

The variables to be used for the AST on Electric load cycling are shown in Table 12.

Table 11 Overview of the constant gas conditions before and during execution of the Electrical Load Cycling AST protocol.

Input	Anode	Cathode
Gas supply	Hydrogen	Air
Stoichiometry	1.5	3.0
Backpressure	0 (ambient pressure)	0 (ambient pressure)
Relative humidity, anode	80% (65°C dew point)	80% (65°C dew point)

Table 12 Overview of variable operating conditions before and during execution of the Electrical Load Cycling AST protocol.

Variables	Low setting	High setting
Cycle frequency	1 cycle per hour	6 cycles per hour
Current density	Cycling between (Mode 2) OCV and 400 mA/cm ²	Cycling between (Mode 1) 200 and 600 or mA/cm ²
Cell temperature	65°C	85°C

4.6 Assessment of results from the Fuel Starvation AST protocol

This AST protocol is the most comprehensively studied protocol in KEEPEMALIVE for single cells. A fraction 2^{3-1} boxed set that was statistically evaluated and reported in the public deliverable (D5.2). A full 2^3 experiment (Table 13) was subsequently performed including post mortem *ex situ* characterization of the MEAs.

Table 13. The factorial 2^3 experimental design incl. one replicate (FS12, Test # 8) which is a duplication of Test #1 (FS02).

Test #	T [°C]	RH [%]	i [mA/cm ²]	name	cycles #	Performance [mV]	decay [mV/h]
01	85	40	400	FS02	100	412	-3.58
02	85	80	400	FS05	50	511	-29.6
03	85	40	200	FS07	700	501	-5.18
04	85	80	200	FS08	80	440	-40.3
05	65	80	400	FS09	250	303	-7.10
06	65	80	200	FS10	500	512	-6.47
07	65	40	200	FS11	875	510	-4.99
08	85	40	400	FS12	250	-----	-----
09	65	40	400	FS14	290	488	-1.44

Three response variables were used in the calculation of effects (as discussed below):

1. The initial (Beginning of Test, BoT) cell performance (at 400 mA cm⁻²) at given test operating conditions
2. The number of fuel starvation cycles conducted, proportional to the test time, limited by the hydrogen gas cross-over current chosen as the End of Test (EOT) criterion.
3. The decay rate from the available UI curves for each experiment. Averaged UP/DOWN voltage data at 400 mA cm⁻² were used.

The voltage stability at 400 mA cm⁻² was found to be 0.49 ± 0.03 V, corresponding to an RSD of 6.1 %. The membrane resistance show an RSD of 18 %.

In order to apply Yates' algorithm for calculation of effects, the experiments were sorted in accordance with **Table 14**. Experiment FS12 (replicate of FS02) was excluded from calculations.

Table 14. Experiments sorted according to Yates algorithm.

T	RH	j	T*RH	T*j	RH*j	T*RH*j	Cycles #	Degradation (mV/h)	name
-	-	-	+	+	+	-	875	-4.99	FS11
+	-	-	-	-	+	+	700	-5.18	FS07
-	+	-	-	+	-	+	500	-6.47	FS10
+	+	-	+	-	-	-	80	-40.3	FS08
-	-	+	+	-	-	+	290	-1.44	FS14
+	-	+	-	+	-	-	100	-3.58	FS02
-	+	+	-	-	+	-	250	-7.10	FS09
+	+	+	+	+	+	+	50	-29.6	FS05

4.6.1 Calculated effects of main operation parameters on BoT cell performance

By means of Yates' algorithm, all effects were calculated as seen in Table 15.

Table 15. Calculation of effects from initial (BoT) performance data (at 400 mA cm⁻²). Columns 3-5 (titled 1-3) are intermediate calculations used by the Yates' algorithm.

Factor	V (mV)	1	2	3	Effects
<i>Mean</i>	412	923	1865	3678	460
<i>T</i>	511	941	1813	225	56.3
<i>RH</i>	501	815	38	201	50.3
<i>T*RH</i>	440	998	187	-390	-97.6
<i>j</i>	303	99	18	-52	-12.9
<i>T*j</i>	512	-61	183	148	37.1
<i>RH*j</i>	510	209	-160	166	41.4
<i>T*RH*j</i>	488	-22	-231	-71	-17.8

The effects show the impact of the input parameters on performance at Beginning of Test (BoT). From T and RH, about 50 mV separates the runs at high and low set point respectively. Current density (j) has a smaller and negative effect. The interactions are generally large; even the way interaction appear to be significant. The largest interaction is found to be T and RH (-97.6). This is illustrated in Figure 18.

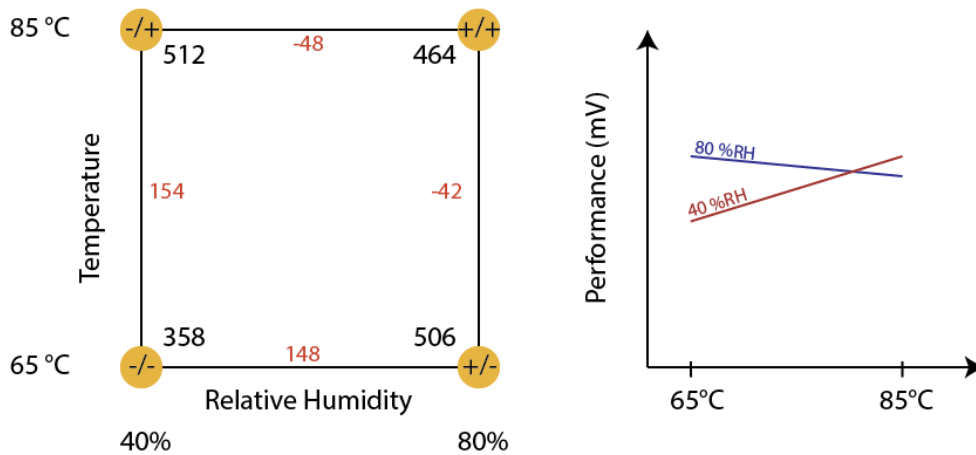


Figure 18. Influence of the T*RH interaction on BoT performance. Corner values (black) indicate averaged responses at given levels. Red numbers indicate averaged effects. Interaction effect is found from half the difference of opposite red numbers.

Figure 18 (left) shows a two-dimensional plot of T and RH. The corner values are the performance average of the two experiments of high and low current density. From the lower left (-/-) corner it can be seen that a large effect in performance is observed by changing either T or RH setting from low to high set-point. They are however not additive: when setting T and RH both high, the resulting performance is lower than the expected contribution from the individual factor. This is caused by the negative interaction between T and RH.

Another way to illustrate this is seen in **Figure 18** (right). Here, the change in performance caused by a change in set-point for temperature is plotted for both settings of RH. The effect of T is clearly affected by the RH set-point: they interact and are thus not additive.

The interpretation of performance data is difficult with relatively small main effects and several significant interactions (**Table 15**). A standard deviation of ~10 mV was estimated for the effects, suggesting that effects should be larger than at least 30 mV (3x SD) in order to be significant. There should of course not be any significant effect of j at BOT, as j is the same for all experiments when comparing performance data at 400mA/cm². And as a consistency check the calculated main effect of j is indeed small, and in the range of the standard deviation. The effect of the interaction RH*j is 41,4mV which is significant (> 3 x SD = 30 mV). An important learning from this assessment is, however, that more parallel experiments should preferably have been conducted for a more robust determination of significance levels.

4.6.2 Calculated effects using #Cycles as response

By means of Yates' algorithm, all effects were calculated as seen in **Table 16**.

Table 16. Main effects calculated from number of Cycles. Columns 3-5 (titled 1-3) are intermediate calculations used by the Yates' algorithm.

Factor	# Cycles	1	2	3	Effects
<i>Mean</i>	875	1575	2155	2845	356
<i>T</i>	700	580	690	-985	-246
<i>RH</i>	500	390	-595	-1085	-271
<i>T*RH</i>	80	300	-390	-255	-64
<i>j</i>	290	-175	-995	-1465	-366
<i>T*j</i>	100	-420	-90	205	51
<i>RH*j</i>	250	-190	-245	905	226
<i>T*RH*j</i>	50	-200	-10	235	59

The main effects of T, RH and j are show negative impact on test duration. From the parallel experiments FS02 and FS12, it was found a standard deviation of 106 cycles. Although limited, this gives some indication of significance levels.

A large, positive interaction is found for RH and j. This effect can be interpreted at half the difference between the average effect of RH at high and low j. This is illustrated in Figure 19.

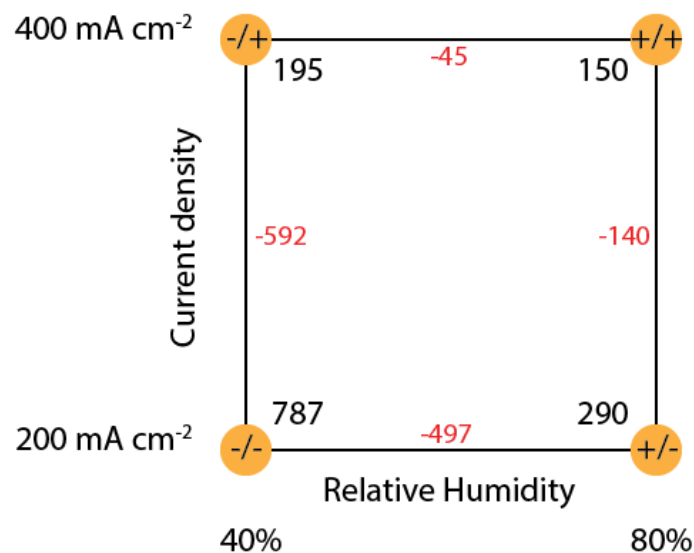


Figure 19. Influence of the RH*j interaction on the number of cycles before cell failure. Corner values (black) indicate averaged responses at given levels. Red numbers indicate averaged effects. Interaction effect is found from half the difference of opposite red numbers.

From the figure it can be seen that the average effect for RH is -45 at high j whereas it is -497 at low j. By analogy, the average effect of j is -140 at high RH and -592 at low RH. Half the difference is in both cases 226 cycles. The effect does not easily translate into a phenomenon of PEMFC degradation nature.

The large interaction of RH and j suggest that the main effects of RH and j are not additive. The isolated effects of RH and j cannot therefore be evaluated without taking the magnitude of the interaction into account.

4.6.3 Calculated effects using decay rate as response

The effects were calculated as seen from **Table 17**.

Table 17. Calculated effects using decay rates. Columns 3-5 (titled 1-3) are intermediate calculations used by the Yates' algorithm.

Factor	Degradation (mV/h)	1	2	3	Effects
<i>Mean</i>	-4.99	-10.17	-56.96	-98.68	-12.3
<i>T</i>	-5.18	-46.79	-41.72	-58.69	-14.7
<i>RH</i>	-6.47	-5.02	-34.04	-68.30	-17.1
<i>T*RH</i>	-40.32	-36.70	-24.64	-54.02	-13.5
<i>j</i>	-1.44	-0.19	-36.62	15.24	3.81
<i>T*j</i>	-3.58	-33.85	-31.68	9.40	2.35
<i>RH*j</i>	-7.10	-2.14	-33.66	4.93	1.23
<i>T*RH*j</i>	-29.60	-22.50	-20.36	13.31	3.33

The main effects of T and RH are large and negative. The effect of j does not appear to correlate with performance decay.

A large interaction between T and RH is also found. The interpretation is illustrated in Figure 20.

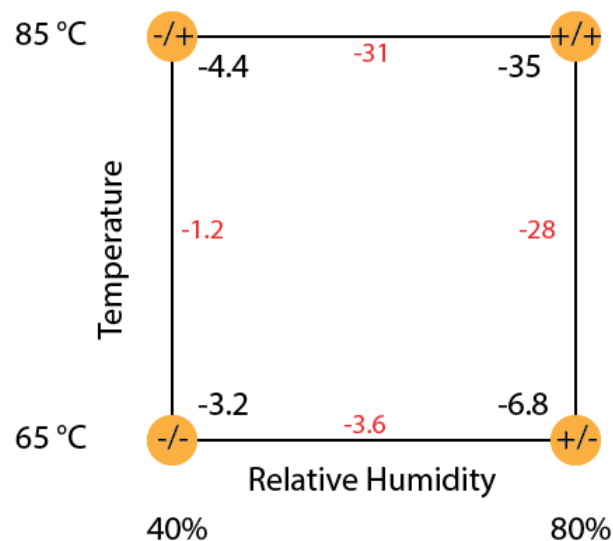


Figure 20. Influence of the T*RH interaction on performance decay. Corner values (black) indicate averaged responses at given levels. Red numbers indicate averaged effects. Interaction effect is found from half the difference of opposite red numbers.

The figure shows that the impact of RH is much higher at high T than at low T (-31 vs. -3.6). It implies from the fact that $T \cdot RH$ is equal to $RH \cdot T$, that the impact of T is higher for high RH.

Again, making assessment of the magnitude of T and RH main effects is difficult when large interaction is documented between the factors. It is plausible that T and RH are coupled in PEMFC. It is also important to recall that a prerequisite for the 2^3 design is orthogonality: that all factors are completely independent of each other.

4.6.4 Interactions of variables in modelling.

The main effects are said to be non-additive when they interact. When interaction is of a significant magnitude (frequently defined as 3 times larger than SD), the interaction must be included in the model.

A model for the response Y containing the interaction term:

$$Y = \beta_1 * T + \beta_2 * RH + \beta_3 * j + \beta_4 * (TxRH) + error$$

where β are the coefficient of the individual main and interaction effects.

4.6.5 Ex-situ analysis of MEA materials subject to ASTing

MEAs aged under fuel starvation conditions were examined by SEM-EDS. Post mortem SEM Backscatter micrographs for two of those MEAs, showing fast degradation during the AST (tests 2 and 4) are shown in **Figure 21**. From the micrographs it is difficult to draw conclusions based on inlet/outlet differences in electrode and membrane thicknesses, therefore the Ru/Pt atomic ratios at anode inlet and outlet are collected in Table 18 alongside the conditions of AST for all the samples.

Table 18. Collected results of Ru/Pt ratios for fuel-starved MEAs.

Test No.	Current density (mA/cm ²)	RH (%)	Temp. (°C)	Number of starvation/recovery cycles	Ru/Pt atomic ratio anode inlet	Ru/Pt atomic ratio anode outlet	Decay (mV/h)
Pristine	N/A	N/A	N/A	N/A	1	1	N/A
5	400	80	65	250	1.04	0.392	-7.10
2	400	80	85	50	0.995	0.284	-29.6
9	400	40	65	290	1.02	0.255	-1.44
1	400	40	85	100	0.841	0.378	-3.58
6	200	80	65	500	0.761	0.258	-6.47
4	200	80	85	80	N.D.	0.336	-40.3
7	200	40	65	875	0.696	0.391	-4.99
3	200	40	85	700	0.476	0.336	-5.18

The results show different trends at the anode inlet and outlet. This difference is expected given the greater degree of fuel starvation at the anode outlet region than at the anode inlet.

At the anode outlet, the Ru/Pt ratio is <1 in the catalyst layer under all AST conditions, indicating that Ru has been lost due to electrochemical corrosion and leaching. Further, the extent of this depletion appears to be strong, and similar in all cases (0.26-0.39), which tends to suggest that the Ru/Pt alloy has possibly reached a new composition stable under the applied AST conditions.

At the anode inlet, the Ru/Pt ratio in the used MEAs ranges from 1 (*i.e.* unchanged compared with the pristine MEA) to 0.476, and the exact ratio within this range appears to depend closely on the applied AST conditions (Table 18), and in particular the extent to which those conditions are expected to lead to a drier MEA. These trends may be clearly seen in **Figure 22**.

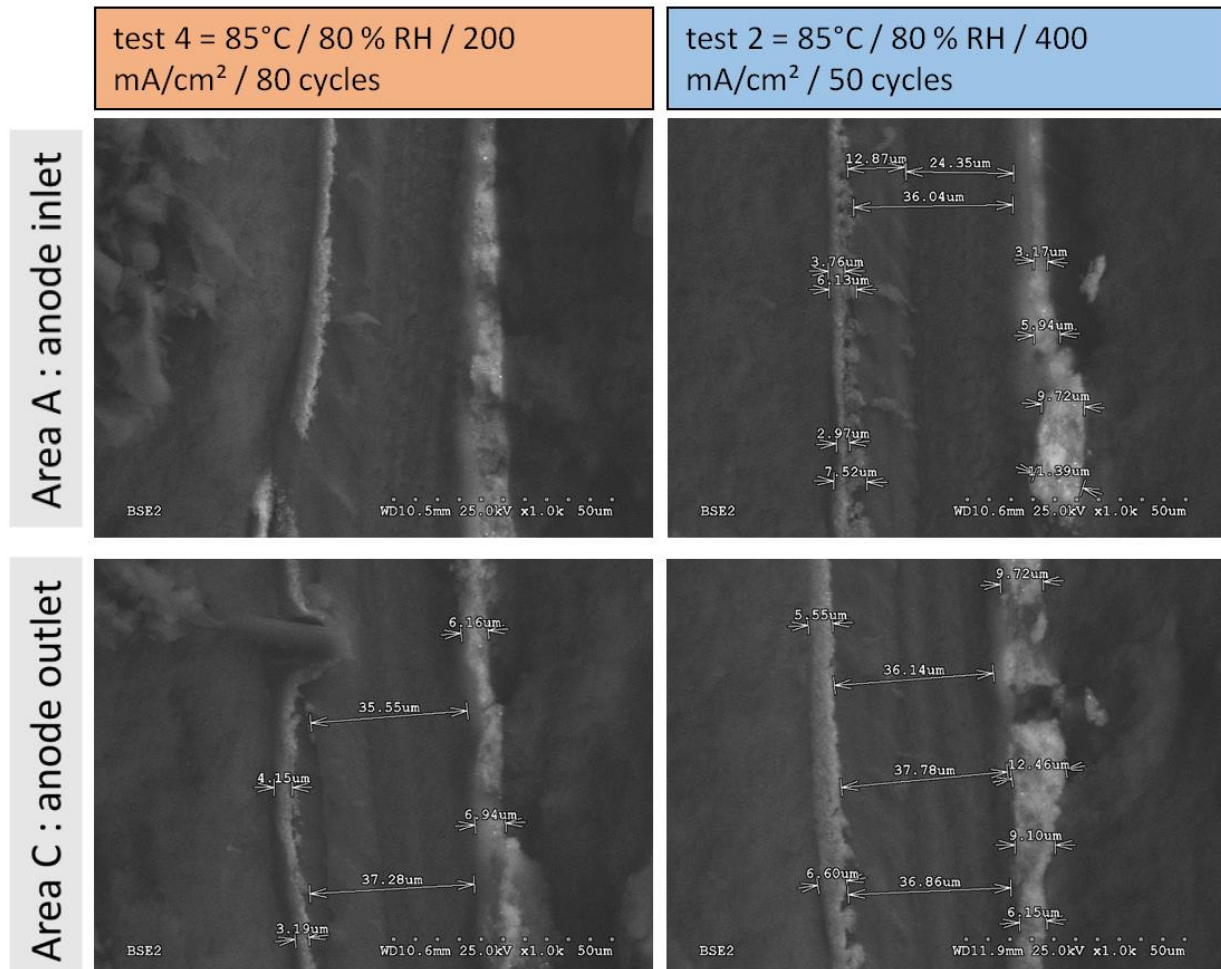


Figure 21. SEM/BS micrographs for tests 2 and 4. Anode side to the left.

The anode catalyst layer composition at the inlet is therefore a sensitive indicator of the combined effects of fuel starvation and the degree of hydration of the MEA on anode catalyst corrosion. Under these conditions, cell reversal effects lead to high anode potential.

These observations are entirely consistent with those demonstrated in the project by *ex-situ* electrochemical characterizations, applying AST load cycling protocols (deliverable report D3.5). The anode catalysts were characterized applying 0.05 – 0.4 V_{RHE} and 0.05 – 1.0 V_{RHE} cycling conditions. An interesting observation is that PtRu/C catalyst did not change its characteristic cyclic voltammogram (CV) profile when the potential was cycled up to 0.4 V. It might suggest that this catalyst keeps its initial surface composition unchangeable over this ageing protocol. The situation is quite different when upper potential was set at 1.0 V. In this case, the characteristic CV for PtRu/C catalyst became similar to the CV profile for Pt/C catalyst. These results suggest that at potentials above 0.4 V_{RHE} the unalloyed Ru starts to be dissolved into the supporting electrolyte, inducing an enrichment of the catalyst surface by Pt. This situation might be also happened during the starvation step.

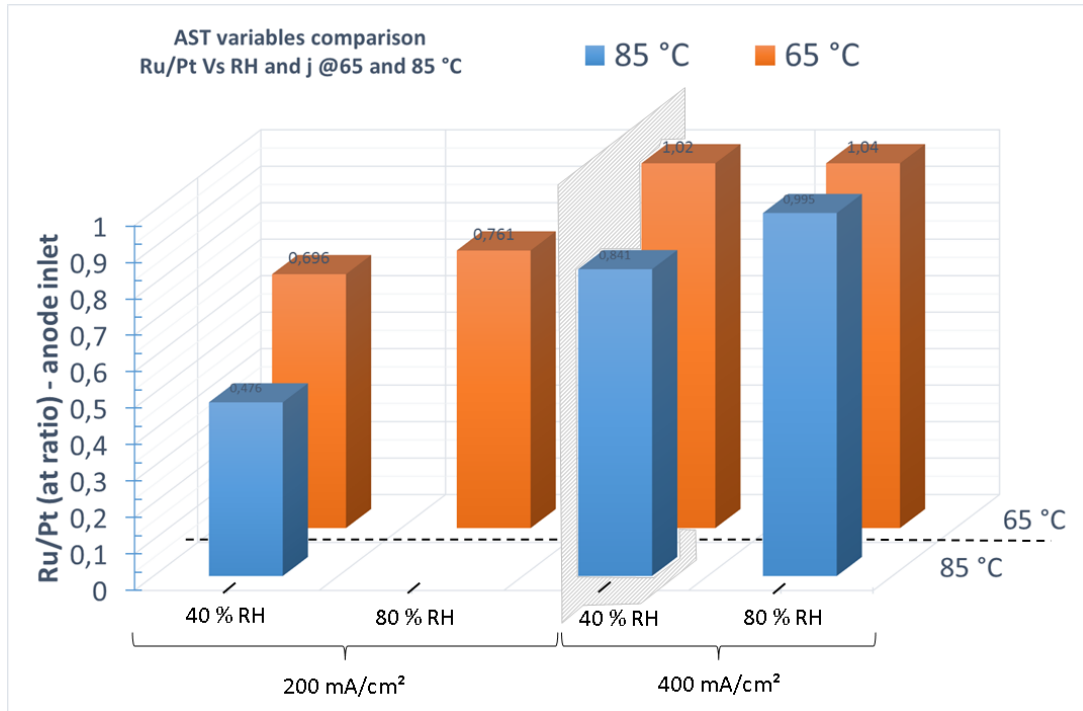


Figure 22. Effect of RH and applied load on Ru/Pt atomic ratio at anode inlet at 65 and 85 °C.

4.6.6 Calculated effects of main operation parameters on Ru:Pt ratio

At the outlet, all eight ratios were used to calculate the effect of the experimental conditions. The effects are summarised in Table 19.

At the outlet, a large effect of RH is found. RH appears to be confounded by T and j: both two-way interaction effects are larger than the main effect of RH. The main effect of T and j at the outlet appear to be small. It is plausible that RH is connected to Ru loss through the solubility in water. The negative effect of temperature could be explained by increased solubility with temperature. The same effect was also found when using number of starvation cycles as response factor (**Figure 19**).

The Ru:Pt ratio determination at the anode inlet region was incomplete, as one measurement was lacking. By inserting an average value of the Ru:Pt ratios measured for the missing figure, effects could be calculated. The result is shown in Table 20.

Table 19. Calculated effects from Ru:Pt ratio at outlet. Columns 3-5 (titled 1-3) are intermediate calculations used by the Yates' algorithm.

Factor	Ru/Pt outlet	1	2	3	Effects
<i>Mean</i>	0.39	0.73	1.32	2.63	0.329
<i>T</i>	0.34	0.59	1.31	0.04	0.009
<i>RH</i>	0.26	0.63	0.02	-0.09	-0.023
<i>T*RH</i>	0.34	0.68	0.02	-0.10	-0.025
<i>j</i>	0.26	-0.06	-0.13	-0.01	-0.003
<i>T*j</i>	0.38	0.08	0.04	-0.01	-0.002
<i>RH*j</i>	0.39	0.12	0.13	0.18	0.044
<i>T*RH*j</i>	0.28	-0.11	-0.23	-0.36	-0.091

Table 20. Calculated effects from Ru:Pt ratio at inlet. Columns 3-5 (titled 1-3) are intermediate calculations used by the Yates' algorithm. * Average value inserted to be able to calculate effects.

Factor	Ru/Pt inlet	1	2	3	Effects
<i>Mean</i>	0.696	1	3	7	0.833
<i>T</i>	0.476	2	4	0	-0.093
<i>RH</i>	0.761	2	0	1	0.149
<i>T*RH</i>	0.833*	2	0	0	0.106
<i>j</i>	1.020	0	0	1	0.283
<i>T*j</i>	0.841	0	0	0	-0.019
<i>RH*j</i>	1.040	0	0	0	-0.062
<i>T*RH*j</i>	0.995	0	0	0	-0.039

The main effect of current density is shown to be dominating. It was verified by testing both a large and small ratio for the missing test 4 that the effect of *j* was still the largest effect. Temperature appears to have a negative, whereas the RH has a positive effect on the Ru:Pt ratio. This is congruent with the results from the ex-situ characterisation of the used MEAs as discussed in Section 4.6.5. The benefit of carrying out the statistical analysis shown above is that the interaction between *T* and *RH* is quantified. These aspects will be further investigated and reported in a planned publication.

The negative effect of *j* and *RH* is not clearly understood. By plotting the cell voltage excursions (Figure 23) upon starvation, there is a significant difference between high and low set-points of *j* in the magnitude of the voltage excursions. It is important to recall how the starvation is simulated by changing the hydrogen stoichiometry from 1,5 to 0.9 during 10 seconds corresponding to an increase in current density of 0.133 and 0.266 at 0.2 and 0.4 A cm⁻² respectively. The higher absolute change in set-point at 0.4 A cm⁻² is suspected cause more severe fuel starvation. The magnitudes of the excursions are not explained by the change in set-point alone, nor are the difference between the high and low excursions explained by the difference of the baseline load. Further, from the higher anode

voltages one would expect the Ru:Pt ratio to decline due to increased dissolution of Ru at high voltages².

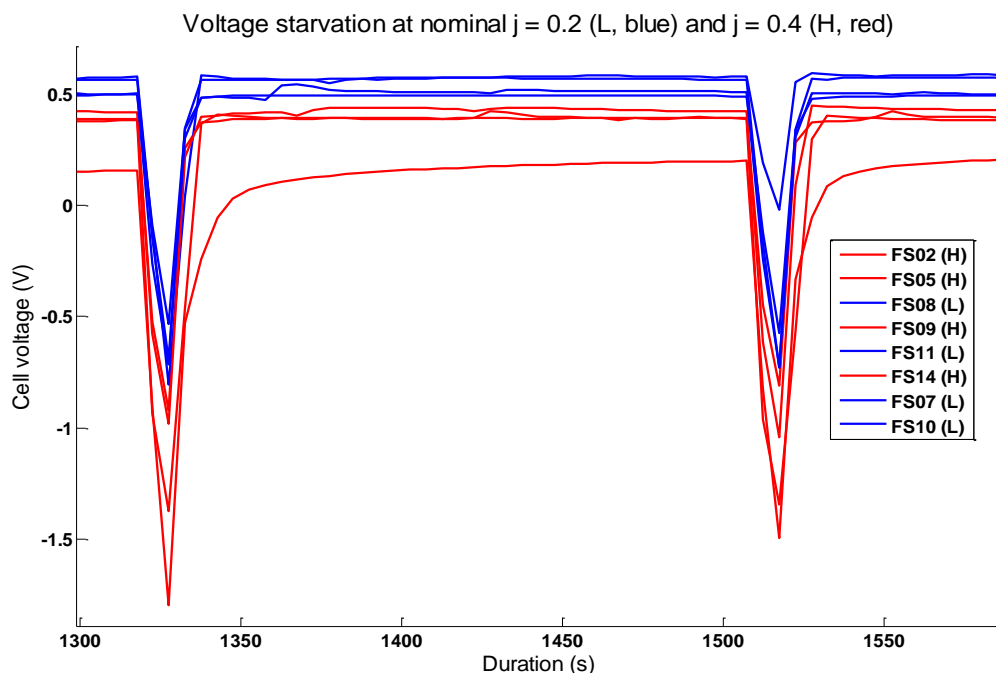


Figure 23. Voltage excursions for eight fuel starvation experiments, blue lines for cells operating at 0.2 A cm^{-2} and red lines for cells operating at 0.4 A cm^{-2} prior to starvation simulation.

For all fuel starvation tests, CO_2 evolution in the anode was detected throughout the execution of the AST protocol. However, to have a comparative picture of the generation of CO_2 and the applied starvation condition, the amount of the CO_2 was calculated during the first 50 (~160 min) starvation/recovery cycles. This number of cycles was selected on the basis of the shortest test (Test No. 2; see also Table 18). The calculations are summarised in Table 21.

Table 21 Emission of CO_2 for various cell tests at low and high current densities.

200 mA/cm ²		Applied Temp. & RH for both j		400 mA/cm ²	
Test No.	*CO ₂ ppm/min	T °C	% RH	Test No.	*CO ₂ ppm/min
4	1989	85	80	2	12017
6	N/A	65	80	5	3548
3	318	85	40	1	2788
7	108	65	40	9	757

*The calculation of CO_2 was done during the first 160 min (~50 cycles) of the starvation protocol.

As it was pointed out above, the higher absolute change in set-point at 400 mA cm^{-2} ($+266 \text{ mA/cm}^2$ compare to $+133 \text{ mA/cm}^2$ at 200 mA/cm^2) may cause more severe fuel starvation. This finding

² See T. Reier, M. Oezaslan, P. Strasser *ACS Catal.*, **2012**, 2 (8), pp 1765–1772.

correlates well with the fact that independent of the applied Temperature and RH, the experiments performed at $400\text{mA}/\text{cm}^2$ generate more CO_2 than those performed at $200\text{mA}/\text{cm}^2$.

Thus, it seems that absolute change in set-point (266 vs. $133\text{mA}/\text{cm}^2$) determines the degree of fuel starvation, due to the different need of fuel (*i.e.* H_2). The more severe starvation will promote side reactions (*e.g.* carbon corrosion, oxygen evolution from water oxidation, etc.) at the anode catalyst to compensate for the lack of fuel, thereby inducing corrosion of the catalyst support and catalyst itself.

As it can be observed in Table 20, RH (water content) seems to rule the side reactions, *i.e.* the corrosion of the catalyst support and/or oxidation of water. Thus, experiments performed at high RH are those which generates more CO_2 (test no. $2 > 5 > 4$); while the experiments performed at low RH are those which generated less CO_2 (test no. $1 > 9 > 3 > 7$). In both cases, the coupling of high Temperature to RH induces higher CO_2 generation. The results may be summarized as follows:

- Degree of fuel starvation is greater at the anode outlet than that at the anode inlet.
- Degradation of the anode inlet depends on the numbers of excursion to high voltages which is governed by the magnitude of current density change during starvation.
- RH and the degree of hydration of anode catalyst governs the catalyst support corrosion.

4.6.7 Current density distribution from segmented cell investigation

A segmented cell was used to determine the current distribution during fuel starvation experiments reflecting the available catalytic sites and hydrogen along the anode channel.

The flow field of the segmented cell is shown in Figure 24 and corresponding cell data for Test 3 is shown in **Figure 25**. During starvation, current distribution is reflecting the available hydrogen in the channel from inlet to outlet. Current distribution during the starvation period appears to be almost stable throughout the 700 cycles. During the recovery interval, the current distribution appears to become less uniform with time. From the UI characterization at $400\text{mA}/\text{cm}^2$, it can also be seen that the current distribution becomes less uniform with time. This is a general trend found for all tests, although it is not most pronounced for Test 3.

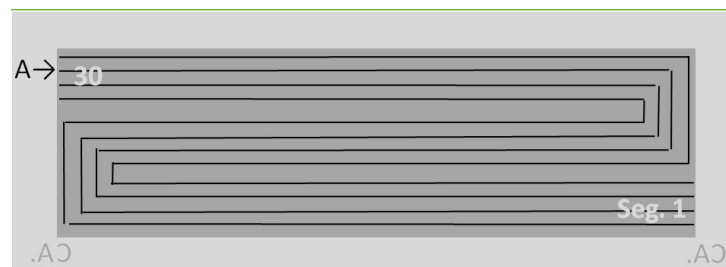


Figure 24 Flow field of the Segmented cell for current distribution measurements, indicating Anode inlet (segment 30) and outlet (segment 1).

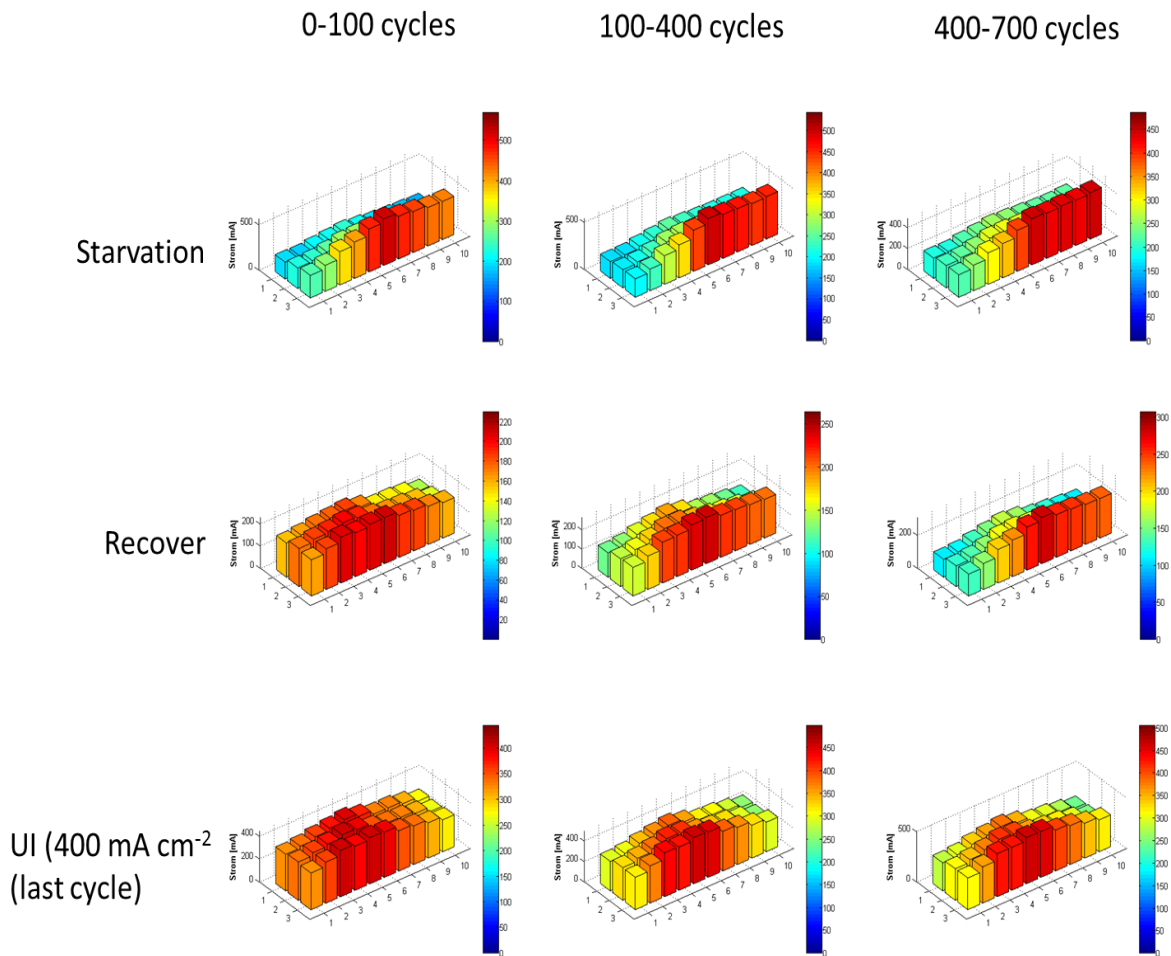


Figure 25. Segmented cell current (mA) distribution for Test 3. Anode inlet is at segment (30 =10, 3) in bottom right corner and anode outlet is in top left corner (segment 1=1,1). Current density during starvation is 333 mA/cm^2 and during recovery 200 mA/cm^2 . Be aware that the max current axis (abscissa, here denoted Strom [mA]) and hence the colour scheme is varying between figures.

It may be seen from **Figure 25** that the current density distribution is similar during the Starvation phase throughout the 700 cycles (upper three plots), whereas during the Recovery phase the current at the different segments vary less between 0 and 100 cycles and more towards the end of the 700 cycles. It is, hence, important to differentiate between the less performing segments during Starvation caused by the lack of hydrogen (as the H_2 is depleted along the channels) and the less performing same segments during the Recovery phase (when there is 50% excess H_2) in which the lower performance of the same segments reflect the actual degradation caused by the previous and repeated fuel Starvations. In the three lower plots of **Figure 25** (obtained during the UI characterisation at 400 mA/cm^2), there is a clear shift of best performing cells towards the centre cell segments. Although it is not evident why we obtain this shift, it might be speculated that it is related to higher gas flow (and hence higher pressure drop) enabling the gas to shortcut and to a lesser degree follow the flow field pattern (Figure 24). If we compare the current density distribution with those for a much faster degrading cell (test 2 which failed after 50 cycles) as is shown in Figure 26, the distribution at the end of this cell's life closely resembles that of cell 3 (**Figure 26**, three lower plots) at close to 700 cycles.

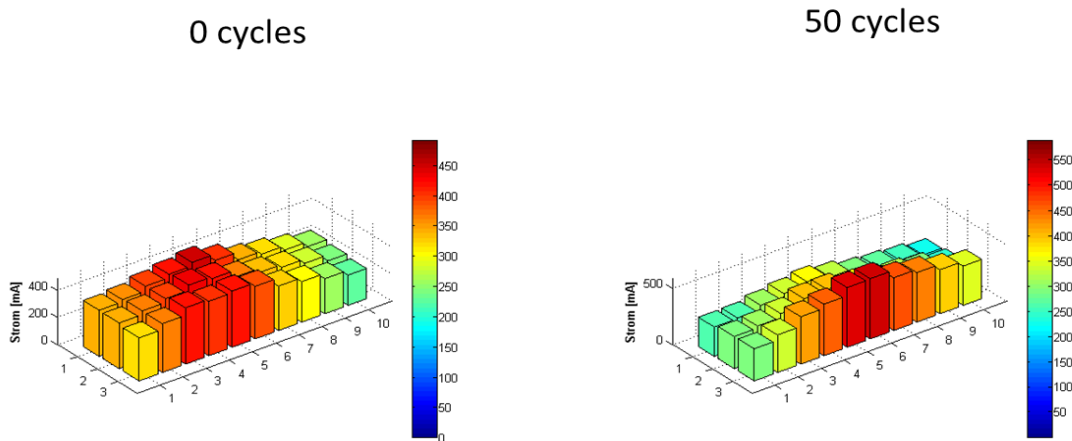


Figure 26. Segmented cell current (mA) distribution during UI (400 mA cm^{-2}) for test 2. Anode inlet is at segment (10, 3) in bottom right corner and exit in top left (segment 1=1,1).

4.6.8 Comparison between fractional 2^{3-1} and full factorial 2^3 experiment

In phase I of the project, a fractional factorial 2^{3-1} experiment was conducted under the fuel starvation protocol. In phase I, two replicated experiments were carried out to estimate variance. In phase II, after revision of the AST protocols, a complete 2^3 experiment was executed. Some changes between the two experiments conducted with segmented cell hardware:

1. In phase I, a non-reinforced membrane was used, whereas a new reinforced membrane material was used in phase II
2. In phase II, the cut-off (cell reversal) voltage of -0.5 V used during phase I was replaced by a 10 second starvation interval, simulated by changing the current density so that the anode stoichiometry was reduced from 1.5 to 0.9 during the starvation period.

The cell voltage profile for the two "-/-" experiments conducted in the two runs are illustrated in Figure 27.

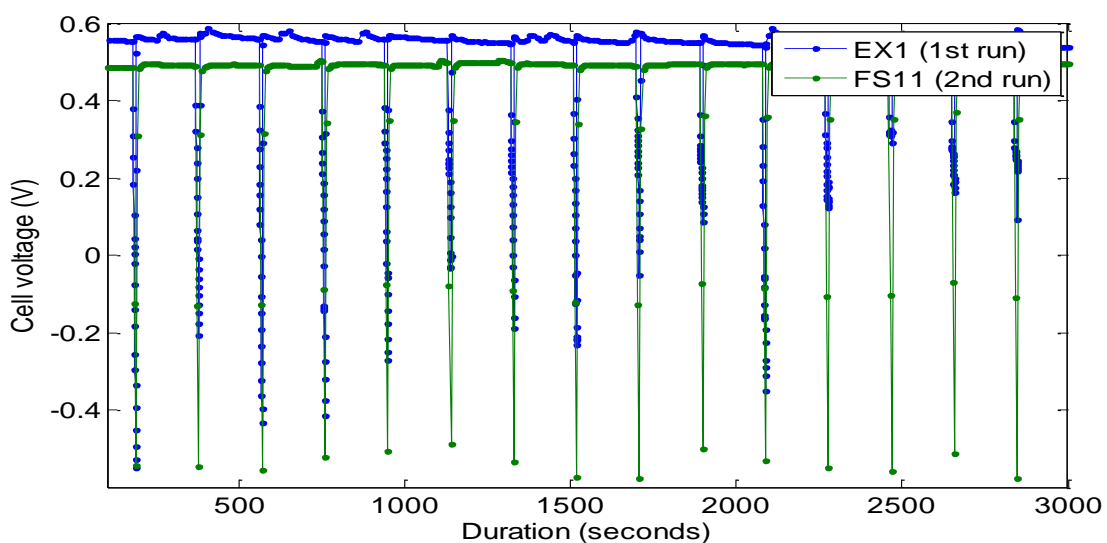


Figure 27. Cell voltage for "-/-" condition experiments (ref)

Table 14).

It appears that the FS11 starvation cycles (phase II) are both longer and causes more severe cell reversal than for EX1 (phase I).

A comparison of the two runs is shown in **Table 22**. Clearly, the second phase exhibits a faster degradation both when it comes to performance and the development of hydrogen cross-over.

Table 22. Comparison of results from Fuel Starvation ASTing between Phase I and II.

T	RH	j	Phase I EXP	No. Cycles	Degradation (mV/h)	Phase II EXP	No. Cycles	Degradation (mV/h)
-	-	-	1	1700	-0.36	FS11	875	-4.99
+	-	-				FS07	700	-5.18
-	+	-				FS10	500	-6.47
+	+	-	4/6	200	-0.69	FS08	80	-40.3
-	-	+				FS14	290	-1.44
+	-	+	3/5	225	-1.92	FS02	100	-3.58
-	+	+	2	1750	-0.18	FS09	250	-7.10
+	+	+				FS05	50	-29.6
Averages				969	-0.79		356	-12.3

The difference in degradation rate is significantly higher for phase II of the AST fuel starvation. The results from phase I were reported in the public deliverable D5.2. It is difficult to find correlations between the results.

When comparing the effect of #cycles, Temperature was shown to have the main impact in phase I. This was not found to be the case in phase II, as seen in **Table 16**. Correlation between runs when using degradation rate to calculate effects is even more difficult due to the unknown magnitude of the two-way interactions in the first run.

From the assessment carried out above, it is concluded the comparable results can only be obtained when materials are kept the same and testing AST protocol is identical.

5 Accelerated Stress Testing of Stacks

When fuel cells are operated in a stack a range of new challenges are faced. There is a range of design criteria that may influence the lifetime of the stack. Important design criteria includes the chosen flow field pattern especially the pressure drop, fuel/air/cooling circuit configuration (U- or Z-flow), and the applied flow configuration (co-, counter- and/cross-flow). Pure hydrogen fuelled stacks/systems are normally operated in dead-end hydrogen mode to optimise the efficiency, while reformate systems are operated in open end fuel configuration ($\square=1.2-1.3$)³. The tests described in the previous part are also relevant for the stack of fuel cells, but it is relative costly to test fuel cell stacks. The stack tests therefore needs to be designed to evaluate the properties related to the stack rather than the individual cell. Some of the suggested tests are straightforward experiments under normal operating conditions, where the initial degradation rate is evaluated. These tests are not real ASTs but serve as a means of comparison to the single cell test and it is hereby established how well the fuel cells perform under real operating conditions compared to the single cell model system.

5.1 Stack Initialisation

All stacks shall be properly initialised and performance characterised prior to execute the test protocols outlined. The single cell break-in procedure (section 4.2, *ibid*) is also recommended for stacks.

5.2 Stack test configuration

From literature it is well known that the optimum flow pattern for a fuel cell stack is Z-flow, where the air/fuel enters in one end and exits in the other. It may, however, be very convenient for practical reasons to operate the fuel cell stack in U-flow configuration e.g. at the cathode as real-life systems most often is equipped with passive humidifiers where the incoming air-stream is being heated and water-exchanged by the exhaust air-stream.

Fuel cell stacks aimed for stationary applications are commonly liquid cooled. In such stacks may a U-flow cooling circuit configuration trap air inside the stack given rise to hot spots. All experiments shall therefore be made with the cooling circuit in a Z-flow configuration, where the liquid enters the stack at the bottom.

5.3 Test parameters

5.3.1 Continuous operation with hydrogen dead-end circuit

The real-life experience from the Vestenskov⁴ field test program has shown that the pure hydrogen dead-end operation causes cross-over development at the hydrogen inlet. The implementation of a reinforced membrane and optimisation of the fuel circuit have proven beneficial for the durability in Vestenskov. However, the effects needs to be quantified and further improvements are possible. The test protocol is outlined in Table 23; the defined stressors concern the purge strategy. The test hours needs to be minimum 1,000 hours per stressor to map out the effects.

³ Cf. Grahl-Madsen et al. (2010): *Overview of real-life operation*. KeePEMalive. internal report D1.1

⁴ Cf. Thor Anders Aarhaug et al. (2012): *Identification of detrimental conditions*. KeePEMalive report D5.2

Table 23 Stack configuration and the dead-end pure hydrogen test protocol.

Input	Anode	Cathode
Gas supply	Hydrogen	Air
Stoichiometry	Stressor: <ul style="list-style-type: none"> Regular purge for ½ s. every 120 s Purge controlled by min. cell voltage. Purge for ½ s when min. $U_{\text{Cell}} < 600$ mV 	2.5
Backpressure	0.4 (1.4 bar pressure) except in purge mode	0 (ambient pressure)
Circuit	Z-flow Co-flow with cooling water	U-flow Co-flow with cooling water
Cooling water temperature	T: 65°C	
Current density	400 mA/cm ²	
Test (hours)	1000 hours per stressor	
Relative humidity	65°C dew point	65°C dew point
Characterization	IU at BoL IU after every 250 test hours IU at EoT At EoT: Leak test & MEA post mortem analysis	

Table 24 Overview of the open-end hydrogen fuelled continuous stack test protocol.

Input	Anode	Cathode
Gas supply	Hydrogen	Air
Stoichiometry	1.2	2.5
Backpressure	0 (ambient pressure)	0 (ambient pressure)
Circuit	Z-flow Co-flow with cooling water	U-flow Co-flow with cooling water
Relative humidity	Dew point 65°C	Dew point 65°C
Cooling water temperature	T: 65°C	
Current density	400 mA/cm ²	
Test (hours)	1000	
Characterization	IU at BoL IU after every 250 test hours IU at EoT At EoT: Leak test at & MEA post mortem analysis	

Table 25 Overview of the open-end reformate fuelled continuous stack test protocol.

Input	Anode	Cathode
Stack orientation	Vertical with air in- and outlet in the bottom	
Gas supply	73% H ₂ , 19% CO ₂ , 8% N ₂ and 20 ppm CO	Air
Stoichiometry	1.2	2.5
Backpressure	0 (ambient pressure)	0 (ambient pressure)
Circuit	Z-flow Co-flow with cooling water	U-flow Co-flow with cooling water
Relative humidity	Dew point 65°C	Dew point 65°C
Cooling water temperature	T: 65°C	
Current density	400 mA/cm ²	
Test (hours)	1000	
Characterization	IU at BoL IU after 250 every test hours IU at EoT At EoT: Leak test & MEA post mortem analysis	

5.3.2 Continuous operation with open-end fuel circuits

The continuous operation tests are straightforward experiments under normal operating conditions, where the initial degradation rate is evaluated. Two protocols are defined for continuous operation one for pure hydrogen operation (Table 24) and one for reformate operation (Table 25).

5.3.3 Start/stop – idle mode stack test protocols

Another very important issue for the fuel cell stack is the start/stop strategy and any actions necessary in the standby period. A fuel cell stack or μ CHP set-up may be started up according to a range of different schemes. In this context it is very important to realise the consequences of the chosen schemes and optimise the strategy. The start-up strategy will partly depend on the choice of idle-mode strategy that again is closely linked to the chosen close down procedure, thus all three strategies needs to be considered jointly.

The system needs to be shut down as gently as possible and several considerations have to be taken when issues during operation or due to lack in demand for heat⁵ require this.

As the system is stopped hydrogen and oxygen is still present in the setup. This situation has some unfortunate consequences as OCV is known to degrade the membrane and cyclic cell voltage in the high voltage range is known to cause catalyst particle agglomeration.

During operation the μ CHP set-up will at times be out of operation e.g. due to lack of heat demand or if operated according to smart grid. During these stand by periods the stack may dry out or in other ways degrade. Three test protocols (Tables 27-29) have been developed to quantify a simple start-stop/idle-mode, a controlled start-stop/ idle-mode, and an emergency start-stop/idle-mode.

⁵ The fuel cell systems in the field test at Vestenskov, Denmark, are regulated on heat demand.

Table 26 Common test parameters for the start/stop protocols (Table 27-29).

Input	Anode	Cathode
Stack orientation	Vertical with air in- and outlet in the bottom	
Gas supply	Hydrogen	Air
Stoichiometry	1.2 (Open-end)	2.5
Backpressure	0 (ambient pressure)	0 (ambient pressure)
Circuit	Z-flow Co-flow with cooling water	U-flow Co-flow with cooling water
Relative humidity	Dew point 65°C	Dew point 65°C
Cooling water temperature	T: 65°C	
Current density	400 mA/cm ²	
Characterization	IU at BoL IU every after 25 start/stop cycles IU at EoT At EoT: Leak test & MEA post mortem analysis	

Table 27 The simple start/stop test protocols.

Step	Parameter	Anode	Cathode
1	Stack loaded	0.4 A/cm ² for 1 hour (cf. Table 26)	
2	Simple shutdown/ idle mode conditions	H ₂ -flow stopped, but H ₂ is left in the fuel circuit at 100 mbar (g). The in- & outlets are blocked	Air supply is stopped, O ₂ slowly consumed. The in- & outlets are blocked at ambient pressure
3	Time (hours)	Time in idle mode: 5 hours	
4	Start-up	Feed gases corresponding to 0.4 A/cm ² are supply Min. OCV > 0.9 V for 30 s Current increased to 0.4 A/cm ² by 0.1 A/cm ² per min	
1/5..		Repeat step 1-4 in total 100 times	
	Characterization	IU at BoL IU after every 25 cycles (step 1-4) IU at EoT At EoT: Leak test & MEA post mortem analysis	

Table 28 The controlled start/stop test protocols.

Step	Parameter	Anode	Cathode
1	Stack loaded	0.4 A/cm ² for 1 hour (cf. Table 26)	
2	Simple shutdown/ idle mode condition	H ₂ -flow stopped, fuel circuit flushed with N ₂ . In- and outlet are blocked at ambient pressure	Air supply is stopped, O ₂ slowly consumed. In- and outlet are blocked at ambient pressure
3	Time (hours)	Time in idle mode: 5 hours	
4	Start-up	Feed gases corresponding to 0.4 A/cm ² are supply Min. OCV > 0.9 V for 30 s Current increased to 0.4 A/cm ² by 0.1 A/cm ² per min	
1/5..		Repeat step 1-4 in total 100 times	
	Characterization	IU at BoL IU after every 25 cycles (step 1-4) IU at EoT At EoT: Leak test & MEA post mortem analysis	

Table 29 The emergency start/stop test protocols.

Step	Parameter	Anode	Cathode
1	Stack loaded	0.4 A/cm ² for 1 hour (cf. Table 26)	
2	Simple shutdown/ idle mode conditions	H ₂ -flow stopped, but H ₂ is left in the fuel circuit. In- and outlet are blocked at ambient pressure	Air flow: 8 NI/min Air dew point: 65°C
3	Time (hours)	Time in idle mode: 5 hours	
4	Start-up	Feed gases corresponding to 0.4 A/cm ² are supplied Min. OCV > 0.9 V for 30 s Current increased to 0.4 A/cm ² by 0.1 A/cm ² per min	
1/5..		Repeat step 1-4 in total 100 times	
	Characterization	IU at BoL IU after every 25 cycles (step 1-4) IU at EoT At EoT: Leak test & MEA post mortem analysis	

6 Lifetime Prediction Modelling

6.1 The initial strategy for KEEPEMALIVE

The initial strategy for lifetime prediction in KEEPEMALIVE was closely linked to the experimental programme of Work Package 2. In order to improve understanding of degradation mechanisms relevant for PEMFC stationary applications, a large number of accelerated stress tests were planned. Extensive online as well as ex-situ characterization was planned for these experiments in order to obtain valuable information on not only overall degradation rates, but also for better understanding of the dominating degradation mechanisms. By using online electrochemical characterization techniques that specifically evaluate degradation of components, information of degradation throughout the test could be compared to post mortem ex-situ characterization that represents the averaged degradation over the test duration.

Statistical evaluation of data from AST protocols would identify the most critical operational parameters for single cells and stacks. Temperature, current density and reactant gas relative humidity was used as variables in most of these ASTs. The acceleration factors of the AST could be estimated from comparison with data for real-life stack running continuously throughout the project duration.

Lifetime prediction is extrapolation of test data to a point in the future where the criterion which classifies End-of-Life is met. For stacks, a performance loss of 10 % is often used for evaluation of durability. In KEEPEMALIVE, the establishment of a prediction model was foreseen to originate from knowledge of degradation rates at component level. These degradation rates would be incorporated into the overall model, weighted by coefficients determined from various operating conditions or events. The stochastic nature of failure is not explained by parametric modelling; statistical modelling of probability of failure is required in order to incorporate this into a lifetime prediction model.

Stack lifetime is more than an average value with an estimate of its variance: lifetime is a distribution. For a 100-cell stack, the failure of one cell is critical for the stack. Thus, the 1 % probability of failure is more interesting than the average failure time of the individual cells. In order to know the 1% probability, information on the distribution of the population must be established. In KEEPEMALIVE, statistical modelling of AST output data was foreseen to establish the weights used for the component or phenomenological degradation rates as well as providing means of analysis of variance. In this way, the uncertainty of the lifetime estimate could be established in addition to the predicted lifetime itself.

6.2 Literature on lifetime prediction

The available literature on lifetime assessment of PEMFC is still limited. The establishment of accelerated stress tests has seen progress, but it remains challenging to correlate acceleration with normal operation. Durability testing and modelling of component testing has been extensively covered, but applying phenomenological modelling for lifetime prediction is challenging; especially since the modelling is often limited to one accelerating factor [1].

6.2.1 Lifetime prediction in batteries

Wenzl et al. [2] proposed to create a matrix of stressing conditions and ageing processes in the battery. In this way, coefficients for correlation between the individual ageing processes and a stressor could be expressed. Due to the expected coupling between factors and processes, it was proposed to use differential rather than a set of linear independent equations. For lifetime models, one alternative presented was to use event based model, where End-of-Life is defined from a fixed number of events. Statistical evaluation of lifetime was however not discussed to be incorporated into models.

NREL has worked extensively with battery life modelling. A semi-empirical model has been established [3] where battery capacity decay and resistance increase is explained from cycling as well as calendar fade. Data from accelerated cycling of the battery is input to the model. Whereas accelerated storage tests are well understood and can be well explained by inverse square time and an Arrhenius temperature dependencies, accelerated cycling tests are poorly understood. Modelling was based on time or #cycle dependency.

6.2.2 Lifetime prediction in fuel cells

Bae et al. [4] has assessed lifetime prediction of direct methanol fuel cells by means of accelerated degradation testing. Temperature was used as stressor and the lowest temperature used as reference when calculating acceleration factors for higher temperature settings. A bi-exponential model was used to fit the performance decay data. The calculated lifetimes were shown to fit well in a Weibull-Arrhenius model. A comparison of estimated lifetime distribution at the lowest temperature based on the higher was compared to the lifetime distribution obtained from the model when using all temperatures was used to indicate the goodness of the lifetime estimates.

In a more recent publication, Bae et al. [5] assessed lifetime prediction of a PEMFC running an accelerated startup-shutdown cycle test, a nonparametric approach to fitting the degradation path was attempted as the bi-exponential approach previously used for DMFC [4] did not fit the data well. Data was fitted with locally weighted least squares with a kernel smoother. Time acceleration factors were obtained from the smoothed curves by a scale-accelerated model, as described by Meeker and Escobar [6]. Compared with the exponential fit, the non-parametric approach was shown to fit the experimental data better. No statistical assessment of lifetime distribution was addressed.

The first paper on the use of reliability data in fuel cell durability testing was published by 3M in 2006 [7]. Here a multicell approach was applied in order to provide lifetime population data. Three stressors were applied. Firstly, three different load cycles were applied: two of them involving OCV excursions while one condition was stationary at nominal load. To evaluate the effect of cell temperature, gas inlet dew points were kept at 70 °C whereas the gas temperature was set for 70, 80 and 90 °C. Interestingly, the failure mode at 70 °C was found to be catalyst degradation whereas at higher temperature membrane integrity failure through hydrogen gas cross-over was observed.

In order to model performance decay, a bi-exponential equation was fitted to the 0.01 A cm⁻² data. The fit was said to be with very good. Interestingly, when trying to estimate lifetime the estimate was hugely dependent on the duration of the accelerated test: The lifetime estimates for 1000 and 3000 hours of accelerated test data was 7100 and 14400 hours respectively.

In order to improve lifetime estimates, statistical modelling was applied. Arrhenius type degradation rate dependency was applied for temperature. For relative humidity, humidity transformation was applied:

$$\text{Humidity transformation} = \frac{RH}{1 - RH}$$

where RH is relative humidity in %. Due to the singularity of RH at 1.0, simulations were done at 0.93. Weibull distribution of the cell populations was assumed. By application of add-on to the statistical software S-PLUS⁶, statistical evaluation of the data was performed. By fitting higher temperature experiments, extrapolation to lower temperatures could be performed.

⁶ S-PLUS is now available on the market as Spotfire.

The same paper put emphasis on a correlation between initial Fluoride Emission Rate (FER) and lifetime. A similar correlation has previously been reported by Baldwin et al. [8], although several publications (reviewed in [9]) has failed to successfully correlate FER with lifetime.

6.3 Lifetime modelling in KEEPEMALIVE

The establishment of a software tool for lifetime prediction has not been achieved in Task 5.4. The main reason for this is insufficient and inconclusive data for an establishment of a model. There are several aspects that contribute to this fact and this is discussed below.

The development of new materials, and changes to new components within the project has rendered much of the data not comparable statistically. These changes have nevertheless been necessary in order to achieve sufficient durability. Especially a change to the reinforced membrane has improved durability. Significant changes to the test programme have also been required. Break-in requirements for the reinforced membrane changed drastically due to the finding that a lot of test data where middle of test performance was better than at beginning of test. Positive degradation rates are of course useless for lifetime estimation purposes.

The use of experimental design for evaluation of stressing conditions is an excellent approach to quantifying the rates of the individual stressors, but also the possible interactions between stressors. The requirement of these 2^3 factorial designs is that all eight experiments need be completed in order to determine the interaction between effects. In KEEPEMALIVE, only a few complete sets have been completed. Statistical analysis of these sets, see D5.2 and 0 in this deliverable, have shown that the magnitude of the interactions are very often large and significant.

An inherent challenge to parametric modelling of degradation is to relate individual degradation mechanism to lifetime. Published work has so far mainly focused on the effect of single stressors: Arrhenius for temperature, humidity transformation and fluoride emission rates to name a few. Multivariate relationships like Eyring have been applied in other applications than PEM fuel cells [10]. The challenge with application of Eyring to KEEPEMALIVE is that the data is not from discrete stressors but a multivariate combination, where interactions are not fully resolved.

The problems associated with the execution of the AST protocols have been the ability to conduct experiments at some combinations of operational set points. This was remedied by introducing introductory scans through all combinations of set points before start of the accelerated stress test. It was further complicated by a change to reinforced membrane that required further revision of the protocol.

It has proven to be challenging to establish an orthogonal set of operating conditions in a 2^3 design. Firstly, the variable space of each stressor must create a significant effect. Significance of results is relative to accuracy of the characterization techniques used. The variable space is limited by the linearity of the effect it creates in addition to remaining orthogonal to the other stressors. Increased insight was obtained throughout the project, but some of the early experimental tests carried out failed to generate significant data. One should therefore be aware of the highly complex relationships and interrelated processes taking place in PEMFCs when interpreting data from the ASTs. One example is the humidity level in the cell, which in fact is affected by both temperature and current density (through the water produced at the cathode).

Due to iterative improvements of materials and challenges in getting reliable data from single cell tests, the stack testing was postponed. Limited testing at stack level has been conducted in KEEPEMALIVE. Several operational problems have been encountered limited the test results thereof to a few protocols. Hence, no complete 2^3 designs have been conducted for stacks. Stacks provide population data through individual cell voltages. A comparison between accelerated and real life data,

which has been abundantly available through the field test project in Vestenskov, to evaluate acceleration factors has not been possible.

Some activities concerning assessment of lifetime has been part of KEEPEMALIVE. One example is the membrane stability in an OCV hold test [11] as shown in Figure 28.

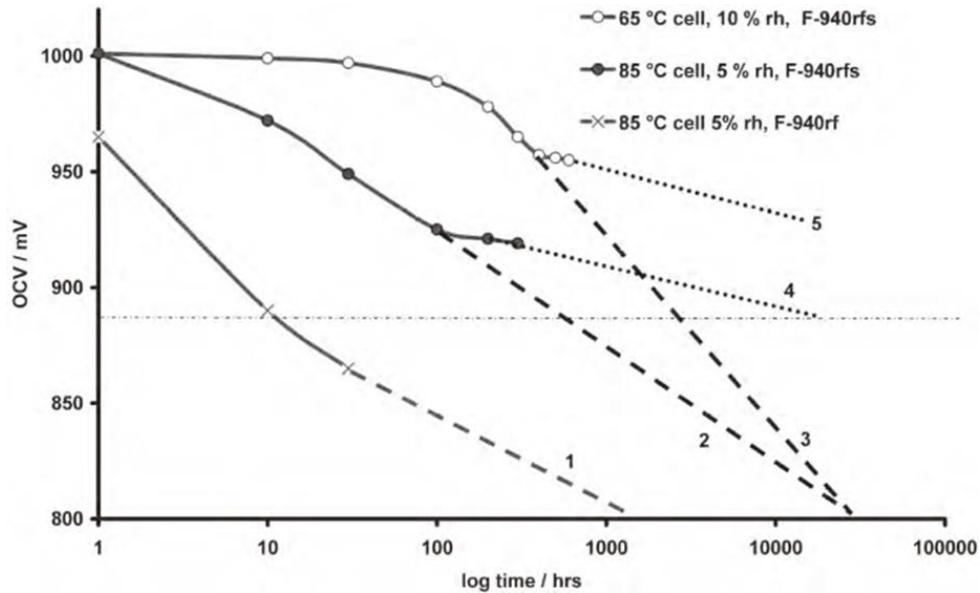


Figure 28 Estimation of membrane's lifetime based on loss of potential during OCV-hold test [11]. Curve 1: Non-stabilised membrane. Curves 2 and 4 are marking the borders of membrane's estimated lifetime at 85 °C. Curves 3 and 5 are marking the borders of membrane's estimated lifetime at 65 °C.

Assessment of IRD lifetime from observed degradation rates has also been. An illustration of the correlation degradation rate, acceptable performance loss and time to End of Life is shown in Figure 29.

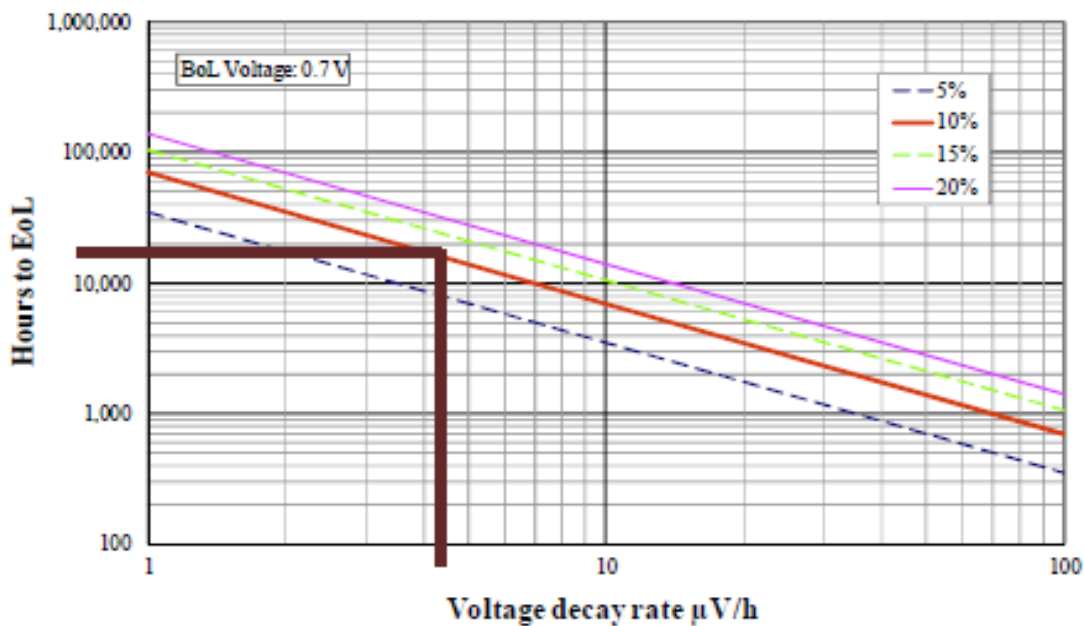


Figure 29. Correlation between degradation rate, acceptable performance loss at End of Life and lifetime.

Despite the failure in the establishment of a tool for lifetime prediction, KEEPEMALIVE has generated a lot of valuable information regarding assessment of lifetime of PEMFC systems. This know-how is processed and summarised in Chapter **Error! Reference source not found.** in terms of a set of recommendations. Here, some of these aspects will be elaborated.

Very little data on statistical significance of test results has been reported in literature. In KEEPEMALIVE, a wide range of issues has been thoroughly addressed in order to evaluate the significance of a result:

1. *At the end of the break-in period of a cell, the variance between cells has been calculated. All effects observed must be larger than this variance in order to be statistical significant.*
2. *The variance for several of the characterization techniques used in this project (i.e., cyclic voltammetry, electrochemical impedance spectroscopy, hydrogen cross-over current) has been established. Knowledge of requirement for significance of effect has been established*
3. *Some parallel experiments have been conducted in order to evaluate variance between experiments beyond beginning of test.*

Through the availability of real life stack data at sufficient resolution (1 Hz logging) and with availability of individual cell voltages, competence in evaluating large data sets has been obtained:

1. *Import and storage of data in a useable format for evaluation*
2. *Efficient smoothing of data, removing noise, yet retaining valuable information.*
3. *Extraction of subsets (i.e., transients) for evaluation of degradation rates*
4. *Evaluation of population distributions*
5. *Fitting of data*

Statistical evaluation of real life stack data has given evidence of a change in cell population distribution from being normal at beginning of life to become better fitted by a Weibull distribution later in stack life. This is an important finding, previously assumed in literature [6,7], that could be utilised for prognostic⁷ purposes (Remaining Useful Life estimate) as well as lifetime prediction.

This competence obtained could unfortunately not be fully utilized in KEEPEALIVE, but will be conveyed to a wider audience in a few planned publications (see 3rd Periodic Report (M31-M42)). With certainty, future projects (possibly funded by the European Commission and through the FCH2 JU) will benefit from this knowledge.

⁷ Relevant for SAPPHIRE (FCH-JU) project.

7 Summary of Experiences from the project

The topic "degradation of fuel cells" is highly complex in its nature. Therefore, a thorough assessment of available literature on the relationships between operation conditions and lifetime issues was carried out leading to definition of an ambitious initial accelerated stress test (AST) program. To realise true collaboration between the involved European research laboratories and industry partners, certain ASTs were intentionally shared between laboratories.

Conditions causing degradation were identified and their relevance for stationary μ CHP applications were verified (WP1). In total 6 stressors were selected to account for the most typical conditions encountered during real life operation of μ CHP units. Operation variables such as Temperature, Relative Humidity (RH), cell voltage and current density were selected as controllable factors for the ASTs. From our best aggregated knowledge, adequate levels of these factors were selected to accelerate the degradation process roughly 100-fold as stated in the DoW.

During the initial phase of the AST program (M1-M25), baseline experiments were carried out at the available laboratories (7 in total) in the consortium, to reveal the inter-laboratory variance. Unfortunately, it turned out that the variation in performance for identical cells tested at different laboratories were substantial. These variations are assumed to be linked to differences in test equipment hardware configurations (e.g., flow fields) and varying active cell area used at the various laboratories (3 to 25 cm²).

Moreover, based on available protocols, experience and recommendations in literature, a break-in procedure was selected and validated to ensure that maximum performance was reached prior to executing the ASTs. In agreement with the DoW, the best available membrane materials were selected (WP4) based on feedback from cell and stack tests (WP2). As new membrane materials were developed, however, we found that the originally verified break-in procedure (for first and second generation membrane materials) was not adequate for the latter generation of membranes (reinforced) (for details, see D 2.2). Thus, revision of the break-in protocol was needed.

Acknowledging the complexity of these relationships, a systematic approach using statistically designed experiments (factorial design) was used, as described in the DoW. To get maximum information out of the factorial designed experiments, complete sets of so-called 2³ experiments (3 factors, each at 2 levels = 8 different operation conditions) were planned at each partner's test facilities. During the execution of those set of experiments, however, it turned out that many of the selected sets of operation parameters led to instable operation (e.g., flooding or dehydration) and several of the 6 distinct AST protocols were not executable. The foreseen statistical analyses to reveal the factor's effect on degradation were, hence, not possible due to incompleteness of the full sets of eight experiments.

Difficulties encountered during the initial iterations of statistical analysis of the data from 37 single cell tests carried out in phase one of the AST program (Month 1-25), lead to the conclusion that only qualitative relationships between factors and degradation could be identified (for details, see D 5.2). As a consequence Stack tests were postponed until reliable single cell characterization could be demonstrated.

During the revision of the initial AST protocols (Months 26-29) four corrective actions were taken, in order to secure more reliable results in the phase 2 of the AST program (Months 30-39):

1. *The number of AST protocols was reduced from 6 to 4, to allow for more replicate experiments and reduce the standard deviation, and thereby, increase the significance of the results from the ASTs.*
2. *No sharing of ASTs between laboratories, due to the high inter-laboratory variation.*
3. *Parameter verification experiments were introduced prior to execution of the revised ASTs to verify that all combinations of parameters lead to stable single cell operation. Further corrective actions to tune the parameters were taken if required, prior to AST execution.*
4. *The duration of the ASTs was reduced from 400 to 200 hours, to allow for more cells to be tested (thereby covering more combination of operation conditions) and be able to complete full sets of factorial experiments with some replicates.*

This way, a more robust approach was taken during phase 2 of the AST program, to assure more reliable and quantitative results, and thereby contributing to generating a sound basis for lifetime prediction modelling (WP5).

8 Recommendations for degradation studies

In this section, we are summarizing the findings from the KeePEMalive project in terms of a set of Recommendations for researchers planning to execute degradation studies on PEMFCs. The list is by no means exhaustive, but should provide valuable hints to avoid pitfalls commonly encountered during execution of such studies.

- 1. Acknowledge that fuel cell operation and degradation mechanisms are complex**
Fuel cells operation include a complex set of inter-related processes which altogether enable these energy converters to convert chemical energy directly into electricity. For low temperature proton exchange membrane fuel cells (PEMFCs), e.g., water plays a key role in membrane proton conductivity and without external humidification of anode gases or sufficient back diffusion of water from the cathode, the ohmic loss will increase dramatically. It is a prerequisite to acknowledge the complexity and reflect it in the scientific approach to be able to reveal the nature of degradation.
- 2. Consider the use of statistical design of experimental program**
Various statistical tools for experimental design are available, and the use of such tools is highly recommended. However, one should consider the tool's adequacy for the given task and pay attention to the inherent assumptions these design tools are based on, and take these into account when interpreting the data.
- 3. Carefully select the stress factors to mimic your fuel cell application**
Stressing factors adequate for your fuel cell application (e.g., μ -CHP, automotive etc.) should be carefully selected based on the typical real life operation profiles. It might be necessary to down-select and try to mimic more than one stress factor by identifying similarities and merging some originally defined stressing conditions.
- 4. Execute adequate baseline experiments as benchmark for AST program**
Carry out baseline experiments with benchmark materials as reference for your AST program every time a precursor or manufacturing technique is changed. An AST protocol will to a certain degree always reflect the specific application and materials in use, although the ultimate goal is a set of generic protocols for wide application.
- 5. Establish a set of End of Test (EoT) criteria for each AST protocol**
In some cases the AST protocol applied causes a steadily decreasing performance, whereas other ASTs eventually cause certain cell failure. The duration of an Accelerated Stress Test until the cell meets your EoT criteria will highly depend on the aggressiveness of the conditions these cells are subject to. EoT criteria may be cell voltage (at a given current density), hydrogen crossover current, cell failure (pin holes) etc.
- 6. Tune the Break-in procedure to ensure maximum performance at BoT**
Activation of fuel cells is highly dependent on the materials in use and the pre-conditioning these have been through during manufacturing and MEA assembly. Some materials need longer break-in to reach maximum performance than others. The Break-in procedure should, hence, be tuned in each case to avoid intermediate peaks in performance during the AST execution.

7. Run parameter verification experiments prior to start ASTs

Stable operation of the fuel cell is a pre-requisite for being able to interpret performance data and determine degradation rates. The parameter span (variable space of the factors (e.g., lower and higher temperature)) should be carefully tuned to assure stable operation. A wide parameter span is beneficial to reveal a significant effect of that factor. However, the larger the span, the required linearity of effects for the factorial designed experiments at 2 levels (Section 2) may be lost.

8. Establish the variance and the statistical significance of your results

Inter-laboratory variance is generally large, primarily related to hardware differences. Splitting the experiments in an AST protocol between laboratories is, therefore, not recommended unless satisfactory variance can be verified. As an integral part of the interpretation effort, a systematic and regular assessment of the variance and statistical significance of the results should be carried out. Only when this is in place, the significance of each factor under study may be verified.

9. Compare to real life experiments for acceleration factor determination

Depending on the application and the corresponding targeted lifetime, an Acceleration Factor (AF) in the range of 10-200 is recommended, corresponding to ASTs with durations of up to 500 hours to enable efficient screening of new materials and assembling procedures. By linking up to already executed or running real life fuel cell field tests, or initiate real life experiments as part of your project, the AF may be determined. In case this is not possible, a reference experiment should be initiated as early as possible, and run continuously in parallel to the AST-program.

10. Distinguish Reversible from Irreversible contribution to performance decay

Performance decay of fuel cells is composed by two terms, the reversible performance decay which may be recovered by applying selected procedures (e.g., voltage cycling to oxidize and thereby remove CO on the catalyst surface) or changing the operating conditions (e.g., increase gas stoichiometries to counteract electrode flooding) and the irreversible performance degradation (e.g., loss of electrochemical surface area (ECSA) of the catalyst or loss in membrane conductivity) which may not be recovered unless the cell components are replaced. When interpreting data from degradation studies, it is important to be aware of this and treat the data correspondingly.

11. Caution should be taken when extrapolating data for lifetime prediction

The degradation rate typically changes significantly over the lifetime of a fuel cell under real life operation as well as throughout the duration of an accelerated stress test. Moreover, there are degradation mechanisms which typically result in certain cell failure (e.g., pin-hole formation), and such factors should be carefully examined and included in cell and stack lifetime prediction. Especially for lifetime prediction of stacks and systems, it is a pre-requisite that the probability of single cell failure is included.

9 References

- [1] Kulikovskiy, A.A., *Analytical Modelling of Fuel Cells*, 1st ed., Elsevier, The Netherlands, 2010.
- [2] Wenzl, H. et. al., *Journal of Power Sources*, 144 (2005) 373-384.
- [3] Smith K, et. al., *Battery Wear from Disparate Duty-Cycles: Opportunities for Electric-Drive Vehicle Battery Health Management, Presented at the 2012 American Control Conference, June 27-29, 2012, Montreal, Canada.*
- [4] Bae, S.J. et. al., *International Journal of Hydrogen Energy*, 35 (2010) 9166-9176.
- [5] Bae, S.J. et. al., *International Journal of Hydrogen Energy*, 37 (2012) 9775-9781.
- [6] Meeker, W.Q. and Escobar, L.A., *Statistical Methods for Reliability Data*, 1st ed., Wiley, USA, 1998.
- [7] Pierpoint, D. et al, *ECS Transactions* 1 (8) 229-237 (2006).
- [8] Baldwin et. al., *Journal of Power Sources* 29 (3-4) 399-412 1990.
- [9] T.A. Aarhaug, "Assessment of PEMFC Durability by Effluent Analysis", PhD Thesis, NTNU, 2011.
- [10] Nelson, W., *Accelerated Testing- Statistical Models, Test Plans and Data Analysis*, Wiley, USA, 2004.
- [11] Klicpera, T, *The Journal of Fuel Cell Technology*, Special issue: Overseas Development Status of Fuel Cells, 13 (1) 2013.

More information can be obtained by contacting the project coordinator:

Dr. Steffen Møller-Holst: steffenh@sintef.no

**This project has received funding from the European Community's
Seventh Framework Programme (FP7/2007-2013) for the
Fuel Cells and Hydrogen Joint Technology Initiative
under grant agreement no.: 245113**

Key KeePEMalive project info:
Start date: 1 January 2010
Duration: 42 months
Cost: €2.9 million
FCH JU funding: €1.3 million

